ACOUSTIC PROPERTIES OF THE SEA FLOOR: A REVIEW

by

Edwin L. Hamilton
Naval Undersea Center
San Diego, California, 92132
U.S.A.

(No Abstract received)

INTRODUCTION

Geologists and geophysicists have two basic roles in underwater acoustics and, especially, in oceanic acoustic modeling. They must study all properties of the sea floor of interest in underwater acoustics, and synthesize these data in order to furnish quantitative information to the acoustician concerned with sound interactions with the sea floor. When data are not available, reasonable predictions may be required. Because of the state of the art, there is insufficient data; therefore, the second important role of the geologist-geophysicist is to make measurements and conduct research in the field of acoustically relevant properties of the sea floor.

At higher sound frequencies, the acoustician may be interested in only the first few meters, or tens of meters of sediments. At lower frequencies, information must be provided on the whole sediment column and on properties of the underlying rock. This information should be provided in the form of geoacoustic models of the sea floor.

A "geoacoustic model" is defined as a model of the real sea floor with emphasis on measured, extrapolated, and predicted values of those properties important in underwater acoustics, and those aspects of geophysics involving sound transmission. In general, a geoacoustic model details the true thicknesses and properties of the sediment and rock layers in the sea floor.

Geoacoustic models are important to the acoustician studying sound interactions with the sea floor in several critical aspects: to guide theoretical studies, to reconcile experiments at sea with theory, and to be able to predict the effects of the sea floor on sound propagation.

The information required for a complete geoacoustic model should include the following for each layer; in some cases, the state of the art allows only rough estimates, in others, information may be non-existent.

1. Properties of the overlying water mass from Nansen casts and velocimeter lowerings.
2. Sediment information (from cores, drilling, or geologic extrapolation): sediment types, grain-size distributions, densities, porosities, compressional and shear wave attenuations and velocities, and other elastic properties. Gradients of these properties with depth; for example, velocity gradients and interval velocities from sonobuoy measurements.
3. Thicknesses of sediment layers (in time) determined at various frequencies by continuous reflection profiling.
4. Locations, thicknesses, and properties of reflectors within the sediment body as seen at various frequencies.
5. Properties of rock layers. Those at or near the sea floor are of special importance to the underwater acoustician.
6. Details of bottom topography, roughness, relief, and slope; for examples, as seen by underwater cameras, and deep-towed equipment.

Among the above properties and information, the basic, minimum information required for most current work in sound propagation is layer thickness, compressional (sound) wave velocity and its attenuation and gradient, and density. Some models require elastic properties such as Lamé's constants. It is the responsibility of the geologist-geophysicist in this field to coordinate his efforts withthose of acousticians in order to supply them with pertinent data, but also to anticipate their future needs.

In 1973, the writer reviewed the present state of the art in acquiring and presenting much of theabove information (Hamilton, 1974a,b). Therefore, some of the following is redundant, or is repeated from the earlier reviews. However, additional, unpublished studies have been done on density and porosity

gradients in the sea floor, on shear wave variations with depth in marine sediments, on sound attenuation versus depth in the sea floor, and on the attenuation of shear waves. Additionally, older figures on sound attenuation are revised, and some new figures are presented on sound velocity gradients based on sonobuoy results. Some new measurements of sediment properties are also presented in partially revised tables.

In the general sections which follow, the information required to form geoacoustic models will be discussed, and, finally, the methods of model construction will be noted.

DISCUSSION OF INFORMATION REQUIRED TO FORM GEOACOUSTIC MODELS

Introduction

The methods used in the field and laboratory to acquire the necessary data for geoacoustic models have been described and discussed in previous reports and in the references in these reports (Hamilton, 1970b, 1971a,b, 1972; Hamilton et al., 1970, 1974). These reports contain, also, numerous references to the results of others, and no attempt is made herein to compile an exhaustive bibliography.

In the discussions which follow, frequent references will be made to the three general environments (Figure 1): the continental terrace (shelf and slope), the abyssal hill environment, and the abyssal plain environment. These environments and associated sediments were discussed in more detail in Hamilton (1971b).

Sediment nomenclature on the continental terrace follows that of Shepard (1954), except that within the sand sizes, the various grades of sand follow the Wentworth scale (noted in Appendix B). In the deep sea, pelagic clay contains less than 30 percent siliceous or calcareous material. Calcareous ooze contains more than 30 percent calcium carbonate, and siliceous ooze more

than 30 percent silica in the form of Radiolaria or diatoms. The Shepard (1954) size grades are shown in these deep-sea sediment types in order to show the effects of grain size.

The averaged results of the writer's measurements and computations to July 1975 are listed in Tables 1 through 6. These tables are revised, in part, from measurements taken since 1973. These data are for the upper 30 cm in the continental terrace where measurements were made in situ with probes, from diver-taken samples, and from cores and other samplers. In deep sea pelagic clay the upper 30 cm of gravity cores and deeper depths in piston cores furnished sediment for measurements. All velocity values are corrected to 23° C and 1 atmosphere pressure (Hamilton, 1971b), using tables for the speed of sound in sea water.

Recent reviews by the writer have bibliographies to about 1973. In the special field of acoustic properties of the sea floor, the reader is also directed to reports in two volumes from Office of Naval Research symposia (Inderbitzen, 1974; Hampton, 1974), and a report by Morton (1975); others are referenced in appropriate, special sections.

Density-Porosity Relationships

General. The equation linking density, porosity, pore-water density, and bulk density of mineral solids in a gas-free system is

$$\rho_{sat} = n\rho_w + (1 - n)\rho_s \qquad (1)$$

where

ρ_{sat} is saturated bulk density

n is fractional porosity (volume of voids/total volume)

ρ_w is density of pore water

ρ_s is bulk density of mineral solids

When sea water is evaporated from sediments during laboratory measurements, dried salts remain with the dried mineral residues. A 'salt correction' should be made to eliminate the false increment to the weight of dried minerals; otherwise, porosity, water content, and bulk grain density values are incorrect. Methods of making a salt correction were detailed by Hamilton (1971b). All values in the tables have been so corrected.

Density of pore water. In computations involving pore-water density, it can be assumed that pore-water and bottom-water salinities are approximately the same. Values for the laboratory density of sea water can be obtained from Sigma-T tables (e.g., NAVOCEANO, 1966). For almost all deep-sea sed-

iments, a laboratory value at 23° C of 1.024 g/cm^3 will be within 0.002 g/cm^3 of any other density at reasonable 'room temperatures'. This value is recommended for laboratory computations. In situ values of water density can be computed from NAVOCEANO tables (1966); such values would vary little (when rounded off) in deep water from those given in Hamilton (1971b) for the Central Pacific.

Density of mineral solids. The bulk density of mineral solids in sediments varies widely because the mineral species present depend on mineralogy and nearness of source areas for terrigenous components, on pelagic particles deposited from the water, and on diagenetic changes in mineralogy in the sea floor.

The geographic variation in pelagic organisms such as diatoms and Radiolaria (silica) and Foraminifera (calcium carbonate) have marked effects on grain density. An average value for grain densities in diatomaceous sediments of the Bering and Okhotsk Seas (Table 2a) is 2.46 g/cm^3, whereas in the open Pacific to the south, the deep-sea clays have average grain density values between 2.68 and 2.78 g/cm^3 (avg. 2.74 g/cm^3).

The averages (g/cm^3) of all samples in each of the three environments (not including diatomaceous and calcareous sediments) are: terrace-2.680, abyssal-hill 'red' clay-2.735 abyssal plain (mostly fine-grained)-2.652. The overall average of the above is 2.693 g/cm^3. Keller and Bennett (1970) report an average for terrigeneous materials of 2.67 g/cm^3, and for the Pacific, 2.71 g/cm^3. Cernock (1970), for the Gulf

of Mexico, reports 2.637 g/cm^3. Akal (1972) reports a general value of 2.66 g/cm^3. In soil mechanics computations a value of about 2.65 g/cm^3 is used for sands and silts when the value is unknown (e.g., Wu, 1966). Thus, there is enough information at hand to predict, with confidence, grain densities for general sediment types.

The conclusion is that the following grain densities be predicted and used in computations when no data is available.

Sediment Type	Avg. Bulk Density of Minerals, g/cm^3
Terrigeneous	2.67
Deep-sea (red clay)	2.72
Calcareous ooze	2.71
Diatomaceous ooze	2.45

Saturated bulk density (or unit wet weight). Averaged values of saturated bulk density for each sediment type within each environment are listed in Tables 1b and 2b. The relationships of saturated bulk density to porosity (Equation 1), not illustrated, are indicated for these data in regression equations in Appendix A. Previous illustrations and discussions indicate the small errors for most sediments when either property is used as an index to the other (Hamilton et al., 1956, 1970b).

In the two deep-water environments, the least saturated bulk density was 1.16 g/cm^3 from the Okhotsk Sea, and the

highest was 1.65 g/cm^3 in a silty layer in Japan Basin turbidites.

In predicting density without any sediment data, one can enter the tables for the appropriate environment and sediment type. In both the abyssal plain and abyssal hill environments, silty clay is the dominant sediment type; there is no significant difference between average densities in these two environments in silty clay: plains-1.333 g/cm^3, and hills-1.344 g/cm^3.

If mean grain size, M_z, is known, a value of density can be derived by entering the diagram or regression equation relating M_z to density (Figure 2).

There is a small (and probably insignificant) correction of laboratory values of sediment saturated density to in situ values. This correction involves an increment to density resulting from more dense water in sediment pore spaces in the sea floor. Laboratory values can usually be used as in situ values, but the correction can be easily made by computing saturated bulk density with equation (1), using in situ density of sea water. The increment to density for most high-porosity sediments varies with water depth, but is only about 0.02 to -.03 g/cm^3 to 6000 m water depth.

Porosity. The amount of pore space in a sediment is the result of a number of complex, interrelated factors; most important are the mineral sizes, shapes, and distributions, mineralogy, sediment structure, and packing of solid grains.

This subject has been previously discussed with many references (Hamilton, 1970b). The interrelated effects of the above factors usually result in a general decrease in porosity with increasing grain size (Figure 3). There is much scatter in the data because of the factors cited above.

The marked effect of mineralogy and environmental control in porosity-density can be seen in the tables and figures: the diatomaceous sediments of the Okhotsk and Bering Seas have significantly higher porosities and lower densities than do similar sediments of the same grain size. Silty clay in diatomaceous ooze has average densities of 1.214 g/cm^3 and porosities averaging 86.8 percent, whereas this sediment type in abyssal hills and other plains have densities around 1.33 g/cm^3 and porosities around 81 percent.

In predicting porosity or density, given the other property (or deriving it by using mean grain size), one can enter density vs. porosity equations or diagrams, but it is usually better procedure to assume values of grain density and pore-water density (laboratory or in situ) and compute the missing property with Equation (1).

Density and porosity versus depth in sediments.- At present it is possible to predict within reasonable limits the density and porosity of sediments at the surface of the sea floor (Hamilton, 1971b), but not at depths greater than can be reached by gravity or piston corers (usually a maximum of about 10 to 20 m). In recent years the Deep Sea Drilling Project has drilled hundreds of holes in the sea floor, and density and porosity measurements have been made

on the cored sediments and rocks. Unfortunately, these measurements cannot account for the increase in volume ("rebound") caused by the removal of the samples from the pressures of overlying sediments ("overburden pressure"). In addition, these density measurements are subject to various errors and must be used with caution.

In an unpublished report (Hamilton, 1975a), special laboratory measurements of density and porosity were combined with other studies to estimate the volumetric increases in sediments removed from boreholes. These data were then used to estimate and illustrate in situ variations of density and porosity with depth in the various important deep-sea sediment types: calcareous ooze, siliceous oozes (diatomaceous and radiolarian oozes), pelagic clay, and deep-water sediments from nearby land sources (terrigenous sediments).

In general, the procedures followed in developing the final profiles and density gradient information were as follows. The best laboratory measurements of density and porosity on Deep Sea Drilling Project (DSDP) samples were selected for the principle sediment types. The volumetric increases, or rebound, in these samples caused by removal from the overburden pressures in the boreholes were estimated from consolidation (compression) tests on similar marine sediments. The in situ porosity profiles were then constructed by subtracting the estimated rebound in porosity from laboratory porosity at various pressures which were converted to depths. In situ density profiles and gradients were then computed from the porosity data.

In Figures 4 and 5, the laboratory and in situ curves of porosity versus depth in the sea floor are illustrated for calcareous ooze and terrigenous sediments. In Figure 6, the variations of density with depth are illustrated for the 5 major deep-sea sediment types. These are generalized examples for the sediment types and no attempt is made to show the scatter of the data. Fine-grained, shallow-water sediments would have a profile similar to the curve for terrigenous sediments.

Some of the other general conclusions of this unpublished study are as follows. There is less reduction of porosity with depth in the first 100 m in these deep-water sediments than previously supposed: 8 to 9 percent in pelagic clay, calcareous and terrigenous sediments, and only 4 to 5 percent in the siliceous sediments. From depths of 300 m the most rebound is in pelagic clay (about 7 percent), and the least in diatomaceous ooze (about 2 percent); calcareous ooze and terrigenous sediment should rebound from 300 m about 4 to 5 percent. Terrigenous sediment, from depths of 1000 m to the surface, probably rebounds a maximum of about 9 percent.

Given profiles of in situ porosity vs. depth in sediments, it is possible to approximate the amounts or volumes of original sediments which have been compressed to present thicknesses by overburden pressures (Hamilton, 1959). This was done for the principle sediment types. To compress to present-day thicknesses of 300 m (the 0 to 300 m interval), it would have required an original thickness of about 420 m of terrigenous sediments, 430 m of calcareous ooze, 440 m of diatomaceous ooze, and 500 m of pelagic clay. Slightly over 2000 m of original sediments would have been required for compression to a present-day thickness of 1000 m of terrigenous sediments.

To estimate the density of a deep sediment layer, the recommended method is to enter (with depths) the density vs. depth curve (Figure 6) for the probable or known sediment type. Determine the density at the top and bottom of the layer and average for a mean density.

The velocity of a deep rock layer is often available from reflection and refraction surveys. To get the mean density of these layers (given velocity) the recommended method is to enter curves relating density and velocity for rocks. At present, the recommended curves are those of Christensen and Salisbury (1975, table 9), Nafe and Drake (1967), and Dortman and Magid (1969).

Compressional Wave (Sound) Velocity

General.- In this section, the better empirical relationships between sound velocity and other properties, and velocity gradients, will be discussed. The empirical relationships are important in predicting sound velocity, but it should be emphasized that wave velocities are elastic properties of the sediment mass. Properties such as porosity and grain size affect sound velocity only in the effects they have on elasticity of the sediment (discussed in Hamilton, 1971a).

Sound velocity and porosity-density relationships. The relationships between sound velocity and porosity have received much attention in the literature because porosity is an easily measured or computed property likely to yield predictable relations with sound velocity. This is because porosity is the volume of water-filled pore space in a unit volume of sediment, and compressional-wave speed is largely determined by the compressibility of pore water, especially in high-porosity silt-clays.

Many studies have emphasized the relationships between sound velocity and porosity over the full range of porosity (Hamilton, 1956, 1970b; Hamilton et al., 1956; Sutton et al., 1957; Laughton, 1957; Nafe and Drake, 1957, 1963; Horn et al., 1968, 1969; Schreiber, 1968; McCann and McCann, 1969; Kermabon et al., 1969; Cernock, 1970; Buchan et al., 1972; McCann, 1972; Akal, 1972;). These studies have included sediments for all of the world's major oceans. The latest data of the writer is illustrated in Figures 7 and 8.

The relationships between sound velocity and density are similar to those for sound velocity and porosity because of the linear relationship between porosity and density.

Sound velocity and grain-size relationships. Grain-size analyses in the laboratory usually include percentages

of sand, silt, and clay, mean and median diameters of mineral grains, and other statistical parameters. The relationships between grain-size and velocity (Figures 9, 10, 11) are in accord with previous studies (Hamilton et al., 1956; Hamilton, 1970b; Sutton et al., 1957; Shumway, 1960; Horn et al., 1968; Schreiber, 1968). Empirically, mean grain size and percent clay size (Figure 11), or percent sand and silt, are important indices to velocity. This is important because size analyses can be made on wet or dry material; and, frequently, size analyses are all the data available in published reports.

Discussion of velocity indices. The information currently available indicates that the higher-porosity silt-clays in the deep basins of the world's oceans have velocities within 1 to 2 percent at any given porosity above about 65 to 70 percent (excluding special types such as diatom and calcareous ooze), at the same temperature and pressure. It is difficult to compare velocity measurements when all have not been corrected to a common temperature, or where temperature is not reported for velocity measurements. Variations in 'room temperature' can easily cause velocity variations on the order of 20 to 30 m/sec (about 1 to 2 percent); variations are much greater if measurements are made in sediment soon after coring or removal from a refrigerator. Temperature measurements should always be made with velocity measurements because temperature variations can cause velocity changes which obscure, and can be greater than,

environmental differences, or differences between sediment types.

If abyssal plain and abyssal hill measurements are lumped together, velocity, at a porosity of 80 percent, from the Mediterranean (Horn et al., 1967; Kermabon et al., 1969), North Atlantic, Caribbean, and Gulf of Mexico (Horn et al., 1968; Schreiber, 1968; Cernock, 1970; McCann, 1972; Akal, 1972), and Pacific and Indian Oceans (Hamilton, this report) averages about 1500 ± 25 m/sec. The lumping of data from various environments and unknown temperatures of measurement is not advised, but the results indicate the small velocity variations in high-porosity sediments of the world's oceans.

As discussed in previous reports, general curves covering the full range of porosity, density, or grain size, wherein data from all environments and sediment types is lumped, should be abandoned in favor of those for particular environments and/or geographic areas or sediment types. In other words, enough data is at hand to quit lumping and start splitting. Examples of this are illustrated in the velocity vs. porosity ~~[velocity-density]~~ diagrams (Figures 7,8). These figures and the tables indicate that at porosities around 80 percent that abyssal-hill silt-clays have lower velocities than do abyssal plain or terrace sediments. The diatomaceous sediments of the Bering Abyssal Plain have significantly higher velocities at higher porosities and

lower densities than either abyssal hill or other terrigeneous abyssal plain sediments (Figure 8).

A resume" of velocity vs. mean or median grain size data indicates that in the various ocean basins, deep-sea sediments of the same mean grain size are apt to have about the same velocities. At a mean grain size of 9.5 phi, the range of velocities from the Pacific and Indian Oceans and adjacent areas (Hamilton, this report), the Gulf of Mexico (Cernock, 1970), the Atlantic, Caribbean, and Mediterranean (Horn et al., 1968, 1969; Schreiber, 1968; is about one percent (about 1495 to about 1510 m/sec).
This is remarkably close considering the lack of temperature control and geographic range. However, as previously discussed in the cases of porosity and density vs. velocity, such lumping should be discouraged. An example, again, is the siliceous sediment of the Bering and Okhotsk Seas. At any given grain size between 8 and 10 phi, these diatomaceous sediments have higher velocities than do the other deep-water sediments (Figure 10).

In the figures, sea-water velocity, if plotted, would be at about 1530 m/sec at 23° C and 1 atmosphere pressure. In the tables, the "Velocity Ratio" (velocity in sediment/velocity in sea water) indicates, quantitatively, the sediment velocity in relation to water velocity. Inspection of the velocity vs. porosity diagrams (Figures 7 and 8), and Tables 1b and 2b, indicate that almost all high-porosity silt-clays from the sediment surface have velocities less than in sea water. This is true in the laboratory and in situ because

the velocity ratio is the same in the laboratory as it is in situ. This interesting relationship results in a small sound channel between the sediment surface and some depth in the sediments depending on the velocity gradient (Hamilton, 1970c).

Prediction of in situ sound velocity at the sediment surface.-

There are three general ways to predict in situ sound velocity at the sediment surface: (1) correct the laboratory velocity from 1 atmosphere pressure and temperature of measurement to the in situ temperature and pressure, using tables for the speed of sound in sea water, (2) multiply the laboratory velocity ratio (sediment velocity/sea-water velocity at 1 atmos., temperature of sediment, and bottom-water salinity) by the bottom-water velocity, or (3) in the absence of sediment data, enter a table (e.g., Table 2b) and select a velocity or ratio for the particular environment and most common sediment type, and then correct to in situ as in (1) or (2), above. The ratio method, (2), is the easiest to apply because the ratio remains the same in the laboratory or in situ, and all one needs for in situ computations is a curve of sound velocity vs. depth in the water mass. These methods were discussed at length (with a numerical example) in a special report concerned with prediction of in situ properties (Hamilton, 1971b).

Compressional Velocity Gradients and Layer Thicknesses

General.- Reflection profiling has become an important tool in geologic, geophysical, and engineering studies. Reflection records indicate sound travel time between impedance mismatches within the sediment or rock layers of the sea floor. To derive the true thicknesses of these layers, it is necessary to measure or predict the interval or mean layer velocity, or to use a measured or predicted sediment surface velocity and a velocity gradient in the sediment body. True thicknesses of layers is a critically important requirement in studies of sound propagation in the sea floor, and in various geological and geophysical investigations. At the present time, the simplest method of measuring layer interval velocities involves the use of expendable sonobuoys. These sonobuoy measurements also provide the basic data for determining velocity profiles and gradients in the sea floor.

The techniques of sediment velocity measurements at sea with expendable sonobuoys, and subsequent data reduction, were developed during the late 1960's (Clay and Rona, 1965; LePichon et al., 1968; Houtz et al., 1968). The results of sonobuoy measurements in the Atlantic, Gulf of Mexico, and Pacific were reported by Houtz et al. (1968). Sonobuoy measurements in the Pacific by Lamont-Doherty scientists have been summarized by M. Ewing et al. (1969) and J. Ewing et al. (1970) for the South Pacific and Coral Sea. Measurements in the North Pacific and Bering Sea have been made by Houtz et al. (1970) and Ludwig et al. (1971); in the Japan Sea (Ludwig et al., 1975a); in the Caribbean Sea (Ludwig et al., 1975b). Measurements have been reported from the Pacific and Indian Oceans, and the Japan and Bering Sea by Hamilton et al. (1974); an example is shown in Figure 12 from the Bay of Bengal. A summary article covering the main ocean basins was published by Houtz (1974). Other references can be found within the cited references, above.

In the discussion in this section, several velocities are involved: (a) instantaneous velocity, V, is the velocity of a compressional wave at any given depth or travel time within the sediment body, (b) mean velocity, or interval velocity, $\overline{V}$, is the average velocity for an interval or layer, and (c) sediment-surface velocity, V_0, is compressional-wave velocity in the sediment just below the water-sediment interface.

Velocity-gradient data for the sea floor are usually produced in the form of linear or non-linear curves based on plots of instantaneous and mean velocity vs. one-way travel time in the sediment or rock layer (e.g., Figure 12).

Velocity gradients. Velocity gradients are usually expressed as an increase in velocity per linear increase in depth, m/sec/m, or sec^{-1}. In the upper levels of deep-water marine sediments these gradients are normally positive, and usually between 0.5 and 2.0 sec^{-1} (Ewing and Nafe, 1963; Houtz et al. 1968; Hamilton et al. 1974). However, most velocity gradients are non-linear if followed to sufficient depths within the sediment body (e.g., Figure 12; Houtz et al., 1968, 1970).

When the velocity gradient, a, is linear, the instantaneous velocity, V, at depth, h, is (Houtz and Ewing, 1963):

$$V = V_0 + ah \qquad (2)$$

At any depth within sediment layers, an average linear gradient, a, can be determined from the parabolic equations for V and $\overline{V}$ vs. t (Houtz et al., 1968, equation 3) by

$$a = (V - V_0)/h \qquad (3)$$

where

V = instantaneous velocity at time t

V_0 = velocity at sediment surface ($t = 0$)

h = layer thickness at time $t = \bar{V}t$

In most sediment sections, the linear velocity gradient decreases with increasing depths, or travel times. The average linear velocity gradient was computed with Equation (3) at increments of 0.1 sec (from 0 to 0.5 sec) for each of 13 areas of mostly turbidite deposition: 4 from Lamont-Doherty investigations (Atlantic, Gulf of Mexico, Aleutian Trench, and Bering Sea-thin), and 9 from Hamilton et al. (1974). The values at each 0.1 sec interval were averaged and plotted in Figure 13. These averaged gradients decreased from about 1.31 sec^{-1} at $t = 0$, to 0.77 sec^{-1} at $t = 0.5$ sec.

As discussed in the next section, such average values can be used to compute a predicted true sediment thickness in many areas where no interval velocity data are available.

The best published data for pelagic, calcareous sediments are summarized in the equations for the Pacific Equatorial Zone (Houtz et al., 1970). Velocity gradients in these thick calcareous sections appear to be higher than the average for turbidite sections: about 1.83 sec^{-1} in the upper levels.

From the same areas, Figure 14 illustrates instantaneous and mean velocity versus one-way travel time of sound in the sediments. From these data one can construct curves of instantaneous velocity versus depth in the sea floor (Figure 15).

In contrast to silt-clays and turbidites, laboratory measurements of compressional wave velocities in water-saturated sands indicates that there is a relatively small, positive gradient with increasing pressure or depth. In computations or predictions of compressional wave velocity versus depth in sands, it is recommended that velocity be increased with the 0.015 power of depth (Hamilton, 1975c).

Thickness computations.- There are three usual alternatives when computing true sediment thicknesses for an area where no interval velocities have been measured: (1) use an equation or curve for mean velocity vs. travel time from a similar area, (2) use a predicted linear gradient and a predicted V_o (discussed below), or (3) assume an interval velocity.

There is now sufficient, published data to show that most areas of turbidites have reasonably close velocity gradients in the upper, unlithified layers. For example, at a one-way travel time of t = 0.2 sec, the computed thickness of a layer using the Atlantic and Gulf of Mexico equations of Houtz et al., (1968), and those for the Central Bengal Fan and Kamchatka Basin (Hamilton et al., 1974) are respectively, 347 m, 341 m,

351 m, and 343 m: a variation of less than 3 percent. Thus, if one is computing sediment layer thicknesses for an area of turbidites where no measurements have been made, the use of equations for the most similar area will probably yield reasonable results. If the sediment type is calcareous ooze, the equations for the Pacific Equatorial Zone (Houtz et al., 1970) are recommended.

Given a linear gradient, a, the sediment surface velocity, V_0, and one-way travel time, t, the thickness of a layer can be computed (Houtz and Ewing, 1963) by

$$h = V_0(e^{at} - 1)/a \qquad (4)$$

where e is the base of natural logarithms

This is a very useful equation because V_0 can be closely estimated (Hamilton, 1971b) and one-way travel time in a layer can be measured from a reflection record; and, as discussed in the preceding section, the velocity gradient can usually be reasonably estimated (Figure 13).

In summary, the following steps are recommended when computing layer thicknesses with Equation (4): (1) measure one-way travel time, t, in the sediment layer from a reflection record; when possible, the measurement should be to 0.001 sec, (2) predict the in situ sediment surface velocity, V_0, using the method discussed by Hamilton (1971b), (3) select a linear velocity gradient for the section depending on one-way travel time (Figure 13); for example, if one-way travel time was 0.25 sec, the assumed gradient

would be 1.0 sec^{-1}, and (4) compute layer thickness, h, with Equation (4).

The third, most popular and least accurate, method for computing layer thicknesses is to measure travel time from a reflection record and assume an interval velocity. These various methods and errors which might be encountered are further discussed in Hamilton et al. (1974).

Attenuation of Compressional (Sound) Waves

Attenuation versus Frequency.

Hamilton (1972) reported the results of in situ measurements of sound velocity and attenuation in various sediments off San Diego. These measurements and others from the literature, allowed analyses of the relationships between attenuation and frequency, and other physical properties. It was concluded that attenuation in dB/ unit length is approximately dependent on the first power of frequency, and that velocity dispersion is negligible or absent in water-saturated sediments. The report also discussed the causes of attenuation, its prediction (given grain size or porosity), and appropriate viscoelastic models which can be applied to sediments. In this section, additional data since 1972 will be noted and briefly discussed.

Figure 16 illustrates a large collection of data on attenuation versus frequency in marine sediments and sedimentary rocks. This figure has been revised from previous publications (Hamilton, 1972, 1974b). The new data include measurements of Meissner (1965), Berzon et al. (1967), Buchan et al. (1971), and Neprochnov (1971). All of the newly-added measurements are indicated with open symbols or dashed lines to indicate the impact of the newer data.

The line labelled "f^1" in Figure 16 indicates the slope of any line representing a first power dependence of attenuation on frequency. It can be

seen that most of the data are consistent with a first power dependence of attenuation on frequency over a frequency range from below 10 Hz to one MHz. The upper and lower bounds of the data plot probably define the area in which most natural marine sediments and sedimentary rocks will lie. With regard to sediment type, the silt-clays, or "mud",(squares) lie in a narrow band along the lower side of the data plot, and the sands (circles), and mixtures such as silty sand, sandy silt, etc., (triangles), lie along the top. These different sediment types are shown on the same plot for convenience. There is no significant difference between sediment types in regard to the relationship between attenuation and frequency. It is interesting to note that Neprochnov (1971) in his summary of a great deal of Soviet data on attenuation in thick layers in the sea floor, remarked that as a rule, a linear relationship was found between attenuation and frequency in the frequency range from 20 to 400 Hz.

In summary, the experimental evidence indicates that the dependence of attenuation on frequency in mud, sand, and marine sedimentary strata, is close to f^1, and does not support any theory calling for a dependence of attenuation on $f^{1/2}$ or f^2 for either (or both) sediment types or mixtures. These data are enough to show that dependence of attenuation on frequency is more nearly f^1 than $f^{1/2}$ or f^2 (but is not enough to verify an exact dependence) for the following: silt-clays, or muds, from a few Hz to at least one MHz, from about 1 kHz to at least one MHz for most sands, and from 150 Hz to one MHz for mixed types. More information is needed for attenuation in pure sands at frequencies below 1 kHz.

Attenuation versus sediment porosity.- The relationships between attenuation and frequency were expressed (Hamilton, 1972) in the form

$$\alpha = kf^n \qquad (5)$$

where

α is attenuation of compressional waves in db/m

k is a constant

f is frequency in kHz

n is the exponent of frequency

The case was made in the preceding section that attenuation is dependent, approximately, on the first power of frequency. If n in Equation (5) is taken as one, the only variable in the equation for various sediments is the constant k. This constant is useful in relating attenuation to other sediment properties such as mean grain size and porosity. The relationships between k and common physical properties give an insight into causes of attenuation, and allow prediction of attenuation.

Assuming that linear attenuation is dependent on the first power of frequency, values of k can be easily computed by dividing attenuation by frequency. This was done for all measurements by the writer and for those in the literature in natural saturated sediments. These values of k were then plotted versus mean grain size and porosity (Hamilton, 1972). Some new data has been added to the figure for sediment porosity vs. k (Figure 17). These measurements are: Tyce (1975): silty clays in the San Diego Trough, and calcareous sediments on the Carnegie Ridge; Muir and Adair (1972): fine sand; Buchan et al. (1971): average of 11 cores in the North Atlantic with less than 5 percent $CaCO_3$; and Igarashi (1973): silty sand off Santa Barbara, California.

The causes of the variations of k (or attenuation) with porosity, as in Figure 17, and with mean grain size, were discussed at length in the original report (Hamilton, 1972, p. 635-643) and will not be repeated here. In general, it was concluded that internal friction between mineral particles was by far the dominant cause of energy losses, and that internal friction varied with the size of grains, the number and kind of grain contacts, and with surface areas of grains in sands, and with cohesion and friction between fine silt and clay particles. In the sands (at porosities less than about 50 %) as grains become smaller, there is a rapid increase in the number of grains per unit volume between porosities of about 45 and 50 percent; additionally the grains become more angular, and there is a marked increase in surface areas in contact. All of these factors result in increased friction between grains which in turn results in greater attenuation of energy from any compressional or shear wave passing through the material. In the mixed sediment types (e.g., silty sand, sandy silt), between porosities of 50 to 55 percent, attenuation reaches a maximum, and with the admixture of finer-grained silt and clay particles, as porosity increases, the larger grains become separated and there is less inter-grain friction. At porosities above about 65 percent, attenuation depends on friction between clay and silt particles, and on cohesion between particles. It is interesting to note that dynamic rigidity varies in the same was as attenuation, as it should if both are mostly caused by friction between grains (Hamilton, 1970a, 1972, 1974a).

The relations between sediment porosity and the constant k (Figure 17) furnish a simple method for predicting attenuation in surficial sediments. The diagram, or regression equations (in Hamilton, 1972, figure 5), can be entered with measured or predicted porosity, and a value of k can be obtained which, when placed in Equation 5, yields an equation useable at

any frequency. A similar figure relating mean grain size and k is in the original report. The values of k so obtained are approximations, but it is predicted that most future measurements of attenuation in marine sediments will result in k values which fall within or near the indicated "envelope." In predicting attenuation, one can use the central (heavy line) values (for which there are regression equations) as "most probable", and the upper and lower dashed lines as indicating "probable maximum" and "probable minimum."

Attenuation versus depth in the sea floor.- For various computations in underwater acoustic and marine geophysics it is necessary to know, or approximate, the average value of attenuation of an interval or layer, or to approximate the gradient of attenuation with depth. Consequently, a collection has been made of available published data on attenuation at the surface and at depth in marine sediments and rocks (Hamilton, 1975b).

As briefly discussed in the preceding section, the relations between the constant k in Equation (5) and sediment physical properties have furnished a useful means of extrapolating measurements and predicting attenuation. The constant k will be used in this section to study the variations of attenuation with depth in the sea floor.

Figure 18 illustrates the available published data (listed and referenced in Hamilton, 1972, 1974b, 1975b, and this report) on the variations of attenuation (expressed as k) at the surface and at depth in silt-clays, turbidites, sedimentary rocks, and basalts in the sea floor. Not shown in Figure 18 are all the values of k for sands and mixed sands and silts; values of k in these materials usually range from about 0.3 to about 0.9 (see Figure 17). Sand bodies in the sea floor are usually relatively thin compared to thick silt-clay and turbidite sections, and the gradients of attenuation in sands are

better known than in silt-clays. All data were recomputed, if necessary, into the form of Equation (5), and then k was computed. Where attenuation was given for an interval or layer, the value is plotted at 1/2 the interval thickness for the first layer, or to the midpoint of a lower layer. As a result, the data in Figure 18 form curves of "instantaneous attenuation" versus depth in the sea floor.

Neprochnov (1971, p. 711) presented attenuation data for thick sediment and rock layers, in the frequency range of 20 to 200 Hz, for 7 areas in the Indian Ocean, Black Sea, and Japan Sea. In Figure 18, the Soviet data are given special symbols. The first layers, which should all be unlithified sediments, are indicated by triangles; the second layers, dominantly sedimentary rock (probably mudstone), are indicated by squares; and the third layers, indicated by diamonds, are sedimentary rock and basalt. These layer identifications are based on Deep Sea Drilling Project sites in the various areas.

Experimental work on attenuation of shear and compressional waves versus pressure in sediments has been largely confined to sands. In these studies, both shear and compressional wave attenuation decreased at about the same rate with increasing pressure. The best data (e.g., Gardner et al., 1964) indicate that attenuation decreases with about the -1/6 power of effective overburden pressure in sands. Curve "B" shown in part in Figure 18, was computed for a fine sand using an average value of k (0.45, off the figure to the right, for 4 stations off San Diego; Hamilton, 1972) at one meter depth and assuming a decrease in k with the -1/6 power of depth. Curve B indicates very rapid decreases in attenuation to about 10 meters, and a less rapid decrease to 150 m (where the computations stopped).

In silt-clays there is probably a distinctly different reaction of attenuation with depth or overburden pressure in the sea floor. The data indicate a probability that attenuation increases with depth from the sediment surface

to some depth where the pressure effect becomes dominant over reduction in porosity. If so, this is a previously unreported finding.

High-porosity silt-clays at or near the sediment surface usually have porosities from about 70 to 90 percent, and k values from about 0.05 to 0.1 (Figure 17). When these sediments are placed under overburden pressures there is a reduction in porosity which would cause an increase in attenuation (Figure 17) as grains are forced closer together and there is more grain contact. At the same time, pressure increases on the mineral frame cause attenuation to decrease as internal friction between grains decreases (grains in harder contact). Thus,under increasing overburden pressure, there should be a progressive increase in attenuation due to reduction in porosity, and a progressive decrease in attenuation due to pressure on the mineral frame. From the appearance of the data plot (Figure 18) it is predicted that the balance of effects is such that attenuation increases with depth in high-porosity silt-clays until a null point is reached. Thereafter, pressure becomes the dominant effect, and attenuation decreases with depth and overburden pressure.

Values and gradients of attenuation in layers in the sea floor can be approximated as follows:

In sands, determine the attenuation at the surface, or predict it from its porosity and Figure 17, and compute the reduction in attenuation at various depths, assuming a -1/6 power-of-depth relationship. If the material is silt-clay, attenuation should increase from a value at the surface to about 100 to 200 m depth (parallel to Curve A in Figure 18) and thereafter decrease gradually with depth as with Curve C.

For sedimentary rocks below about 400 m, use Curve C to establish

values of k. For basalt layers below the sea floor, use a value of k established from laboratory and field experiments: 0.02 to 0.05; a value of 0.03 is recommended (full references in Hamilton, 1975b).

Impedance

The characteristic impedance of a medium is the product of density, ρ, and velocity, V_p (impedance = ρV_p, $g/cm^2 sec$); it is an important property of any material. The amount of energy reflected (or lost) when sound passes from one medium into another of greater impedance is largely determined by impedance difference, or "mismatches" (e.g., Kinsler and Frey, 1962). In the field of marine geophysics, echo-sounding and continuous-reflection-profiling records indicate the travel-time of sound between impedance mismatches at the particular power and frequencies involved in the sound source, and in amplifying and filter systems. Most deep-water surficial sea-floor sediments have sound velocities less than that in the overlying bottom water, but the echo-sounder records strong reflections in these areas because sediment densities are so much greater than water densities that a sufficient impedance mismatch is created.

Average impedances were computed for the sediments of this study (Tables 3 and 4), using the averaged, measured values of sediment density and velocity in Tables 1b and 2b. Figures and regression equations in Hamilton (1970b,d) illustrate the relationships between impedance and porosity and density.

Laboratory impedances require corrections to in situ values. The methods of correcting laboratory density and velocity to in situ values were noted above; the in situ impedance is merely the product of the corrected values.

Rayleigh Reflection Coefficients and Bottom Losses at Normal Incidence

The computations of Rayleigh reflection coefficients and bottom losses at normal incidence, herein discussed, are a simple, straightforward procedure, given accurate values of density and velocity for sediment and water. Comparisons of such computations with actual measurements at sea (Hamilton, 1970d) by Breslau (1965, 1967) and Fry and Raitt (1961), and the measurements and computations of Hastrup (1970, p. 183-184, figure 5) demonstrate that the method is valid and yields realistic predicted values for acoustic bottom losses (dB) at the water-sediment interface given certain restricted conditions.

The whole subject of reflection, refraction, and energy losses of sound incident on the sea floor is too complex for simple statements and is the subject of other papers in this symposium. The reader is cautioned against attempted use of Rayleigh reflection coefficients and bottom losses except under very restricted conditions of bottom sediment layering, sound energy levels, and frequency. In general, the Rayleigh fluid/fluid model is valid only when, for various reasons, any second or other layers in the sea floor cannot reflect sound which interferes with that reflected from the water-sediment interface (see Cole, 1965 for discussion). As discussed in the paper by Bucker and Morris (this symposium) more sophisticated models of reflectivity and bottom loss involve layers and varying layer properties (Bucker, 1964; Bucker et al., 1965; Cole, 1965; Morris, 1970; Hastrup, 1970; Hanna, 1973).

Rayleigh reflection coefficients and bottom losses at normal incidence were illustrated by Hamilton et al. (1956) and are the subject of a separate paper (Hamilton, 1970d). For the present report, the values of Rayleigh reflection coefficients and bottom losses (Tables 3 and 4) were computed using average density and velocity values in Tables 1b and 2b, plus values of water density and velocity, and appropriate salinity, at 23° C; the normal-incidence equations under Table 3 were used in these computations. As discussed in the

1970d report, laboratory values of reflection coefficients and bottom losses at normal incidence are so close to corrected, in situ, values, that laboratory values can be used as in situ values in generalized studies.

Figures in Hamilton (1970d) illustrate the empirical relationships between porosity and density and Rayleigh reflection coefficients and bottom losses at normal incidence; regression equations are included in the cited report.

Elastic and Viscoelastic Models for Marine Sediments

The subjects of elastic and viscoelastic models for water-saturated porous media, and measurements and computations of elastic constants in marine sediments have been discussed in six recent reports (Hamilton, 1971a,b, 1972, 1974a,b; Hamilton et al., 1970). Some general conclusions are noted below, but the reader should consult, especially, the 1971a, and 1972 reports for fuller discussions, supporting data and detail, and numerous references to the literature on the subject, and the work and opinions of others. Other references are in the symposium volume edited by Hampton (1974).

In soil mechanics and foundation engineering, and in some fields of physics and geophysics, the Hookean model and equations are commonly used in studies of wave velocities and the elastic constants in sediments and rocks. Although the Hookean equations adequately account for wave velocities in most earth materials, they do not provide for wave-energy losses. To account for both wave velocities and energy losses, various anelastic models have been studied or proposed.

In older literature it was possible to consider such models as the Maxwell or Kelvin-Voigt viscoelastic models and others, for wave propagation in earth materials, where the sparse data were made to fit models by use of arbitrary constants. In the past decade there has been enough research in earth materials to indicate restrictive parameters for any anaelastic model.

Given macroscopic isotropy, small, sinusoidal stresses, wave lengths much greater than grain size, and frequencies from a few Hertz to at least several hundred kHz (and probably in the MHz range for most natural sediments), the restrictive parameters for any elastic, 'nearly elastic', or viscoelastic model for marine sediments can be summarized as follows: (1) almost no marine sediments can be considered suspensions, (2) almost all have non-spherical mineral particles which form structures which have sufficient rigidity to transmit shear waves, (3) Poiseuille flow (through small tubes) probably does not hold for relatively impermeable silt-clays nor for natural sands, (4) velocity dispersion is absent or negligibly present, and (5) the dependence of attenuation on frequency is close to f^1. Some relative movement of pore water and mineral frame cannot be excluded on the basis of present evidence, although the above parameters indicate that, if present, it should be small.

The model proposed below is within, or accounts for, the above restrictions, and has several advantages. It is a good working model which does not specify the mechanics of attenuation. It is an anelastic model which includes provision for velocity dispersion and non-linear dependence of attenuation on frequency; the user is thus not committed, a priori, to no-velocity-dispersion or to any particular f^n relationship. The model also indicates clearly those factors involving velocity dispersion and non-linear attenuation which, if negligible, can be dropped. It indicates clearly under what conditions Hookean elastic equations can be used to in-

terrelate wave velocities and other elastic moduli. And interestingly, this model has been widely used in studies of rocks and the earth's crust, as well as in the properties of polymers, and in some soil mechanics studies.

It should be emphasized that other models are not excluded if they are within the above stated parameters. The whole subject merits much more experimental and theoretical study.

A model and concomitant equations within the parameters noted above is a case of linear viscoelasticity. The basic equations of linear viscoelasticity have been summarized in an excellent treatise by Ferry (1961). For the model recommended in this paper, the basic equations (Adler, Sawyer, and Ferry, 1949) have been discussed in different form, including neglect of negligible factors, by Nolle and Sieck (1952), Ferry (1961, p. 93-94), Krizek (1964), White (1965), Krizek and Franklin (1968), Hamilton et al. (1970), and others.

In the above model, the Lamé elastic moduli μ and λ are replaced by complex moduli, $(\mu + i\mu')$ and $(\lambda + i\lambda')$, in which μ,λ, and density govern wave velocity and the imaginary moduli, $i\mu'$ and $i\lambda'$ govern energy damping. The following (Ferry, 1961, p. 11-13) illustrates the stress-strain relations in this model. For a sinusoidal wave, if the viscoelastic behavior is linear, the strain will be out of phase with stress.

The stress can be vectorially decomposed into two components: one in phase with strain and one 90° out of phase. For a shear wave, the complex stress/strain ratio is $\mu^* = \mu + i\mu'$. The phase angle, Φ, which expresses energy damping is, in this case: $\tan \Phi = \mu'/\mu$.

The basic derivations of the above model are in Ferry (1961) and White (1965) and will not be repeated here. Without assumptions as to negligible factors, the equations of the model in the form of Bucker (in Hamilton et al., 1970, p. 4046), or in Ferry (1961, p. 94, 419), reduce to the following for both compressional and shear waves (with some changes in notation).

$$\frac{1}{Q} = \frac{aV}{\pi f - \frac{a^2V^2}{4\pi f}} \qquad (6)$$

where

1/Q is the specific attenuation factor, or specific dissipation function

a is the attenuation coefficient

V is wave velocity

f is frequency (circular frequency, $\omega = 2\pi f$)

Subscripts (p or s) can be inserted into Equation (6) when referring to compressional or shear waves.

When energy damping is small (i.e., $\lambda' \ll \lambda$ and $\mu' \ll \mu$: White, 1965, p. 95; Ferry, 1961, p. 123: $r \ll 1$, where $r = aV/2\pi f$), the term in the denominator of Equation (6), $a^2V^2/4\pi f$, is negligible and can be dropped. This leaves the more familiar expression (e.g., Knopoff and Macdonald, 1958; White, 1965; Bradley and Fort, 1966; Attwell and Ramana, 1966):

$$\frac{1}{Q} = \frac{aV}{\pi f} \qquad (7)$$

$$\frac{1}{Q} = \frac{2aV}{\omega} = \frac{\Delta}{\pi} = \tan \phi \tag{8}$$

$$\Delta = aV/f, \text{ or } a = \Delta f/V \tag{9}$$

Additionally

$$\frac{1}{Q_p} = \tan \phi_p = \frac{\lambda' + 2\mu'}{\lambda + 2\mu} \tag{10}$$

$$\frac{1}{Q_s} = \tan \phi_s = \frac{\mu'}{\mu} \tag{11}$$

$$\frac{\Delta E}{E} = \frac{2\pi}{Q} \tag{12}$$

$$\alpha = 8.686a \tag{13}$$

Where (in addition to those symbols already defined)

Δ is the logarithmic decrement (natural log of the ratio of two successive amplitudes in an exponentially decaying sinusoidal wave)

$\tan \phi$ is the loss angle

$\Delta E/E$ is fraction of strain energy lost per stress cycle

α is attenuation in dB/linear measure (e.g., dB/cm)

Equations involving compressional - and shear-wave velocities in Hamilton et al. (1970), or in Ferry (1961), are (in Ferry's notation)

$$(\lambda + 2\mu) = \rho V_p^2 (1 - r^2)/(1 + r^2)^2 \tag{14}$$

$$\mu = \rho V_s^2 (1 - r^2)/(1 + r^2)^2 \tag{15}$$

where

$r = aV/2\pi f$, λ = Lame´'s constant, μ = rigidity, ρ = density

In Equations (14) and (15), the term, $(1 - r^2)/(1 + r^2)^2$, indicates the degree of velocity dispersion for linear viscoelastic media. When damping is small (defined above), this term is negligible, and can be dropped, as implied by Ferry (1961, p. 94). This leaves the more familiar Hookean equations

$$(\lambda + 2\mu) = \rho V_p^2 \tag{16}$$

$$\mu = \rho V_s^2 \tag{17}$$

This means that if the factor $(1 - r^2)/(1 + r^2)^2$ in Equations (14) and (15), and the term in the denominator of Equation (6), $a^2V^2/4\pi f$, are considered negligible and dropped, that wave velocity, 1/Q, and the log decrement are independent of frequency, and linear attenuation is proportional to the first power of frequency.

Computations with the data of Hamilton (1972), and from the literature, indicate that most water-saturated rocks and sediments qualify under the above definitions as media with 'small damping'. For example, computations from Hamilton (1972, table 1) indicate that the factor $(1 - r^2)/(1 + r^2)^2$ for compressional waves at 14 kHz is 0.9992 in fine sand, and an average of 0.9997 for 4 silty clays; in Pierre shale (McDonal et al., 1958), the factor for shear waves is about 0.992. Equations (7) through (13), (16) and (17) should apply to both water-saturated sediments and rocks.

Those investigators who wish to include velocity dispersion and 1/Q or a log decrement dependent on frequency, and linear attenuation not proportional to the first power of frequency, can consider Equations (6), (14), and (15). The results of computations involving wave velocities, densities, and associated elastic constants will be negligibly different if one uses viscoelastic Equations (6), (14), and (15), or the classic Hookean elastic Equations (e.g., Equations 16 and 17.).

→ Computations of Elastic Constants →

The computation of elastic constants for saturated sedi-

ments was discussed at length in Hamilton (1971a), and was reviewed in Hamilton (1971b, 1974). The general subject will only be briefly noted in this section.

To compute elastic constants in saturated sediments using Hookean elastic equations, as justified in the preceding section, requires values of density, and any two other constants. Density and compressional velocity are easily measured or can be reasonably predicted for most common sediment types (Hamilton, 1971a,b,1974). One more elastic constant is required to compute the others. The third constant selected (Hamilton, 1971a) to use in computations was the bulk modulus (incompressibility). The theoretical basis of this computation follows Gassmann (1951).

Gassmann (1951) formulated a 'closed system' in which pore water does not move significantly relative to the mineral frame (no movement of water in or out of a unit volume), the effective density of the medium is the sum of the mass of water and solids in a unit volume, wave velocity and energy damping (e.g., 1/Q) are independent of frequency, and Hookean elastic equations can be used in studying wave velocities unless energy damping is to be considered. The closed system as a special case in the elasticity or viscoelasticity of saturated, porous media, has been noted in many studies (references in Hamilton, 1972).

The bulk modulus was selected as the third constant to use in computing the other elastic constants because it appears possible to compute a valid bulk modulus from its com-

ponents. The equation used in this computation (Gassmann, 1951) is

$$K = K_s \frac{K_f + Q}{K_s + Q} \qquad Q = \frac{K_w(K_s - K_f)}{n(K_s - K_w)} \qquad (18)$$

where,

K_s = aggretate bulk modulus of mineral solids

K_f = frame bulk modulus ("skeletal" bulk modulus of Gassmann, 1951)

K_w = bulk modulus of pore water

n = decimal-fractional porosity of sediment.

Good values for the bulk modulus of distilled and sea water, K_w, and most of the common minerals of sediments, K_s, have been established in recent years. This leaves only a value for the frame bulk modulus, K_f, needed to compute a bulk modulus for the water-mineral system.

A contribution of Hamilton (1971a) was in derivation of a relationship between sediment porosity and the dynamic frame bulk modulus. Using this relationship, the frame bulk modulus was derived for each sample, and used with the bulk moduli of pore water and minerals to compute the system bulk modulus with Equation (18). The expectable excellent relations between porosity and the bulk modulus are shown in Figure 19.

The computed bulk modulus, and measured density and compressional-wave velocity were then used to compute the other elastic constants. Those equations using these three constants were favored. The equations are

$$\text{Compressibility, } \beta = \frac{1}{\kappa} \tag{19}$$

$$\text{Lamé's constant, } \lambda = \frac{3\kappa - \rho V_p^2}{2} \tag{20}$$

$$\text{Poisson's ratio, } \sigma = \frac{3\kappa - \rho V_p^2}{3\kappa + \rho V_p^2} \tag{21}$$

$$\text{Rigidity (Shear) Modulus, } \mu = (\rho V_p^2 - \kappa)3/4 \tag{22}$$

$$\text{Velocity of shear wave, } V_s = (\mu/\rho)^{1/2} \tag{23}$$

Tables of measured and computed elastic constants for various sediment types are in Hamilton (1971a); up-dated tables are in Hamilton (1974a) and in this report (Tables 5, 6). The decimal places do not indicate accuracy, but are merely listed for comparisons. The values of the elastic properties listed should be regarded as approximations and predictions for comparison with future measurements.

The values for the elastic constants in the tables and figures are for 23° C and 1 atmosphere pressure. These can be used in some basic studies, but cannot be used as in situ values because density, velocity, and the bulk modulus all require corrections from laboratory to in situ. Such corrections with a numerical example are in Hamilton (1971b).

Shear Wave Velocities, Gradients, and Attenuation

Near-surface velocities of shear waves.- The bulk moduli, k, of the deep-water sediments are plotted against density X (velocity)^2, or ρV_p^2, in Figure 20. When a material lakcs rigidity, k = ρV_p^2. A line representing k = ρV_p^2 is also plotted in Figure 20. Assuming these are true values of k, the consistent divergence of the data from the line indicates the presence and approximate values of rigidity, μ ($\rho V_p^2 = k + 4/3\mu$). In Figure 8 (porosity vs. velocity), almost all points are well above Wood's equation for a suspension, which also indicates the presence of appreciable rigidity. The conclusion that almost all natural marine sediments have enough rigidity to transmit shear waves is supported by such laboratory measurements and computations, and by actual in situ measurements.

The computed values of shear wave velocities for the various sediments are listed in Tables 5 and 6. The least values of shear velocity (170 to 190 m/sec) are in deep-water clays in the abyssal plain and abyssal hill environments, and the highest values (470 m/sec) in continental terrace fine sands.

The computed values in the tables are comparable to values measured in situ. A survey of the literature indicates that near-surface shear wave velocities in water-saturated sands vary from 50 to over 500 m/sec (e.g., Cunny and Fry, 1973; Hamilton et al., 1970; White and Sengbush, 1953; Shima et al., 1968; Kawasumi et al., 1966; Barnes et al., 1973). Some measured, in situ, near-surface shear wave velocities in silt-clays ("muds"), include: 30 m/sec in a tidal mud flat near Monterey, California (Lasswell, 1970); 90 m/sec in San Francisco Bay mud (Warrick, 1974); 50 to 190 m/sec in deep-sea pelagic sediments in the Indian Ocean (Davies, 1965); 137 m/sec in silty clay on land (Cunny and Fry, 1973); 100 to 300 m/sec in silt in Japan (Kudo and Shima, 1970; Shima et al., 1968).

Shear wave velocity versus depth in marine sediments.- A recent, unpublished report (Hamilton, 1975c) reviewed the available data concerning the variations of shear wave velocity with depth in sands and in silt-clays.

The shear wave velocity measurements in sands included 29 selected in situ values at depths to 12 m (Figure 21). The regression equation for these data is $V_s = 128(D)^{0.28}$, where V_s is shear wave velocity in m/sec, and depth, D, in m. The data from field and laboratory studies indicates that shear wave velocity is proportional to the 1/3 to 1/6 power of pressure or depth in sands; that the 1/6 power is not reached until very high pressures are applied; and that for most sands, the velocity of shear waves is proportional to the 3/10 to 1/4 power of depth or pressure. The use of a depth exponent of 0.25 is recommended for prediction of shear velocity vs. depth in sands.

The shear velocity measurements in silt-clays and turbidites included 47 selected, in situ measurements to depths of 650 m (Figure 22). The shear velocity gradient in the upper 40 m ($4.65\ sec^{-1}$) is 4 to 5 times greater than is the compressional velocity in comparable sediments. At deeper depths, shear velocity and compressional velocity gradients are comparable.

Attenuation of shear waves (general).- There is an interesting approximation of the relations between attenuation and velocity which has been derived from Equations (10) and (11) with the assumption that bulk viscosity, k' ($k' = \lambda' + 2/3\mu'$) is zero; resulting in: $\lambda' = -2/3\mu'$ (Kolsky, 1963; Vasil'ev and Gurevich, 1962; De Bremaecker et al., 1966). Substituting for λ' in Equation (10), and then substituting $\mu' = \mu/Q_s$ (Equation, 11), $\mu = \rho V_s^2$, and $(\lambda + 2u) = \rho V_p^2$, yields

$$\frac{Q_p}{Q_s} = 0.75 \frac{V_p^2}{V_s^2} \qquad (24)$$

All of the cited authors, above, noted that Equation (24) is not in accord with the sparse experimental data.

De Bremaecker et al. (1966) set $\lambda' = 0$ for sedimentary rocks, which leads to

$$\frac{Q_p}{Q_s} = 0.50 \frac{V_p^2}{V_s^2} \tag{25}$$

which these authors believed more in accord with the experimental data.

The few available values (measured and computed) for the numerical coefficient in Equations (24) and (25), for saturated marine sediments, indicate it to be much less than 0.75 or 0.50; more in the range of 0.03 to 0.2.

Because of the many uncertainties and assumptions involved in computing shear wave energy losses using Equations (24) or (25) (or variations thereof), it is considered a better method at this time, in the absence of measurements, to use logarithmic decrements, Δ_s, and the ratio of compressional wave decrement to shear wave decrements, Δ_p / Δ_s to approximate values of shear wave attenuation. The relationships between the logarithmic decrement and the attenuation coefficient are shown in Equations (8) and (9).

Logarithmic decrement of shear waves (sands).- Literature values of the logarithmic decrement of shear waves in sands range mostly from 0.1 to 0.6 for laboratory and in situ studies; most values lie between 0.2 and 0.4. There are very few measurements of Δ_p / Δ_s. One of the best in situ studies using shear waves, was that of Kudo and Shima (1970) who derived a logarithmic decrement value of 0.39 for diluvial sand in Tokyo. Kudo and Shima (1970) also found that the attenuation of shear waves was approximately proportional to the first power of frequency, and that there was no velocity dispersion in the range of 30 to 80 Hz. Meissner (1965) measured Δ_s as 0.125 to 0.325 (avg. 0.25) in situ in diluvial sand and clay. Barkan (1962) reported damping ratio, D, values which convert to values of Δ_s between 0.3 and 0.4 ($\Delta_s \approx 2\pi D$). Both Seed and Idriss (1970) and Whitman and Richart (1967) have used

damping ratios equivalent to $\Delta_s = 0.31$ for sands and other sediments. In summary, if values of shear wave energy losses in sands are required for computations, a value of $\Delta_s = 0.3$ can be assumed and used with shear wave lengths to derive values of attenuation (e.g., with Equations 8, 9, and 13).

Logarithmic decrements of shear waves (silt-clays).- Values of logarithmic decrement in silt-clays vary from about 0.1 to 0.6, as in sands. The best values are probably in the range of 0.1 to 0.3 (Molotova, 1966; Zhadin, in Vasil'ev and Gurevich, 1962; Richart et al., 1970; Barkan, 1962; Kudo and Shima, 1970). Whitman and Richart (1967) and Seed and Idriss (1970) have used damping ratios of 0.05 ($\Delta_s = 0.31$) for silt-clay soils. The few literature values of Δ_p / Δ_s are about 0.2 to 0.3. When computing values of shear wave attenuation in water-saturated clay, Berzon et al. (1967) chose a value of 0.3 for Δ_p / Δ_s. It is recommended that if approximate values of attenuation of shear waves are desired for silt-clays, that a value of $\Delta_p / \Delta_s = 0.3$ be assumed, and Δ_s computed after reducing measured or predicted compressional wave attenuation to Δ_p using Equations (13) and (9). After Δ_s is derived, shear wave attenuation can be computed from Equations (9) and (13).

Shear wave attenuation in shale and mudstone.- Very little information is available for in situ shear wave attenuation in shales and mudstones. The two best known to the writer are studies of compressional and shear waves in the Pierre shale (f = 20 to 125 Hz) and in mudstone in Japan (15 to 90 Hz). McDonal et al. (1958) measured the following in Pierre shale:

$\Delta_p \approx 0.087$, $\Delta_s \approx 0.324$, and $\Delta_p / \Delta_s \approx 0.27$.

Shear wave attenuation in dB/m in Pierre shale is about 10 times greater than compressional wave attenuation. Kudo and Shima (1970) measured shear wave velocity and attenuation in Tertiary mudstone in Tokyo. These values were $V_s = 420$ m/sec, $Q_s = 6.5$, and $\Delta_s = 0.48$.

Shear wave attenuation versus frequency.- The little information presently available indicates that shear wave attenuation, as compressional wave attenuation, is dependent on the first power of frequency (e.g., Kudo and Shima, 1970; McDonal et al., 1958). Some of the shear wave energy-loss data previously referenced can be placed in the form of Equation (5), where the attenuation of shear waves, α_s is in dB/m, and frequency, f, is in kHz. Examples computed by the writer are:

Material	Equation	Reference
Diluvial sand	$\alpha_s = 13.2f$	Kudo and Shima (1970)
Diluvial sand and clay	$\alpha_s = 4.8f$	Meissner (1965)
Alluvial silt	$\alpha_s = 13.4f$	Kudo and Shima (1970)
Water-saturated clay	$\alpha_s = 15.2f$	Molotova (1966)
Tertiary mudstone	$\alpha_s = 10.1f$	Kudo and Shima (1970)
Pierre shale	$\alpha_s = 3.4f$	McDonal et al. (1958)

Comparisons of the attenuation of compressional and shear waves (in dB/m) indicate that, in the few cases available, shear wave attenuation is on the order of 10 to 20 times greater than compressional wave attenuation.

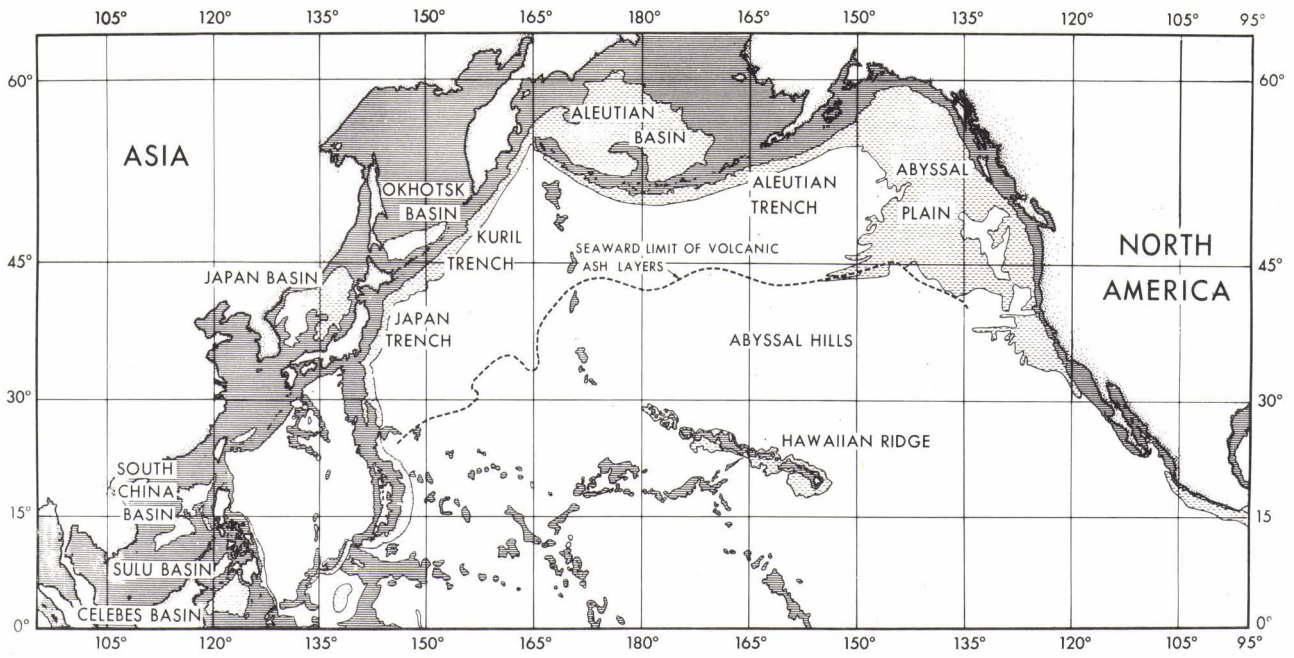

FIG. 1 PHYSIOGRAPHIC PROVINCES AND RELATED ENVIRONMENTS, NORTH PACIFIC AND ADJACENT AREAS. SEAWARD LIMIT OF VOLCANIC ASH LAYERS FROM HORN ET AL (1969). THE THREE GENERAL ENVIRONMENTS ARE CONTINENTAL TERRACE (SHELF AND SLOPE): SOLID, HORIZONTAL LINES; ABYSSAL PLAIN (TURBIDITE): HORIZONTAL, DASHED LINES; AND ABYSSAL HILL (PELAGIC): WHITE AREAS.

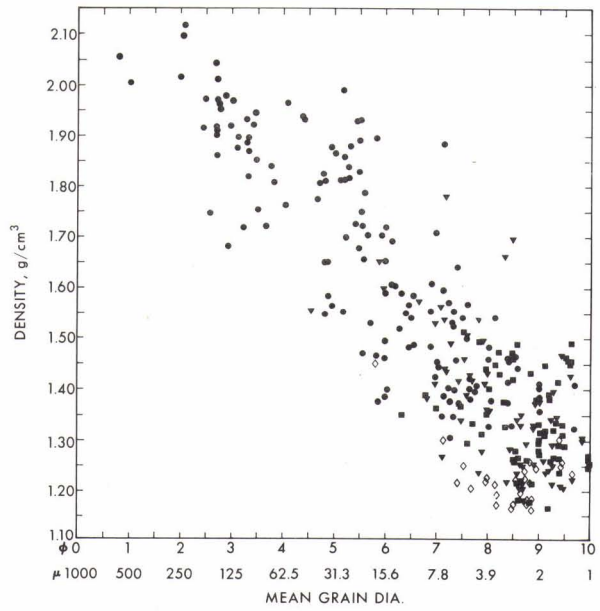

FIG. 2 MEAN DIAMETER OF MINERAL GRAINS VERSUS DENSITY. ROUND DOTS ARE CONTINENTAL TERRACE (SHELF AND SLOPE) SAMPLES; SQUARES ARE ABYSSAL HILL SAMPLES; TRIANGLES ARE ABYSSAL PLAIN SAMPLES; OPEN DIAMONDS ARE DIATOMACEOUS SAMPLES FROM THE BERING AND OKHOTSK SEAS.

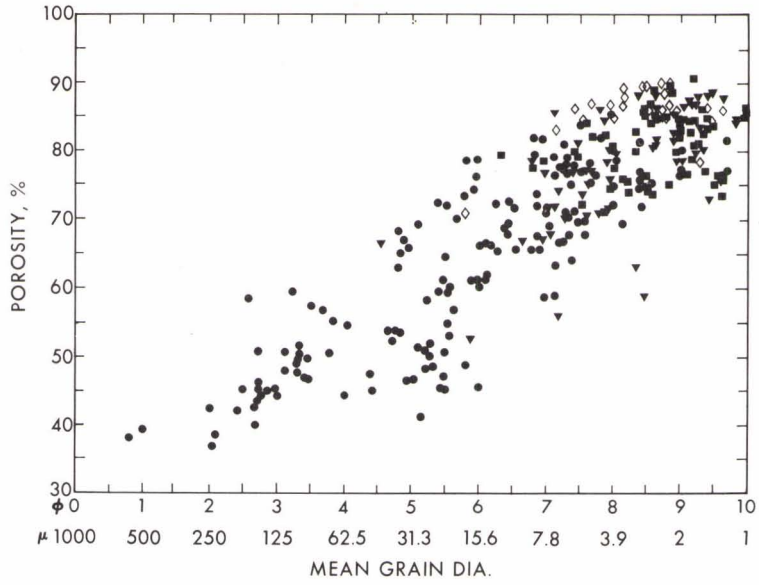

FIG. 3
MEAN DIAMETER OF MINERAL GRAINS VERSUS POROSITY, ALL ENVIRONMENTS; SYMBOLS AS IN FIGURE 2.

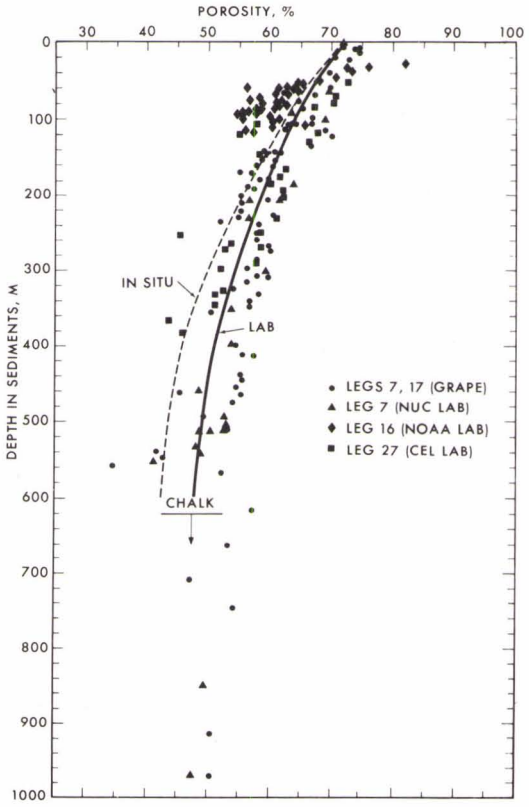

FIG. 4
POROSITY VERSUS DEPTH IN CALCAREOUS SEDIMENTS, CENTRAL PACIFIC. SYMBOLS ARE LABORATORY VALUES FROM THE DEEP SEA DRILLING PROJECT. DERIVATION OF THE IN SITU CURVE EXPLAINED IN THE TEXT.

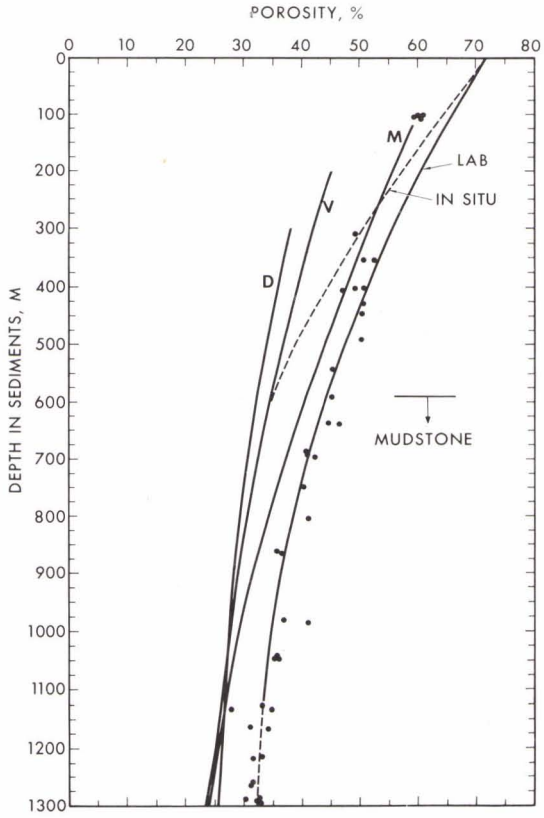

FIG. 5
POROSITY VERSUS DEPTH IN TERRIGENOUS SEDIMENTS. DOTS ARE LABORATORY VALUES FROM DEEP SEA DRILLING PROJECT SIZE 222 IN THE ARABIAN SEA. CURVE "D": GULF COAST SHALE (DICKINSON, 1953); CURVE "V" IS SHALE FROM VASSOEVICH (IN RIEKE AND CHILINGARIAN, 1974, p. 40, Fig. 16); CURVE "M": MUDSTONE IN JAPAN (MAGARA, 1968).

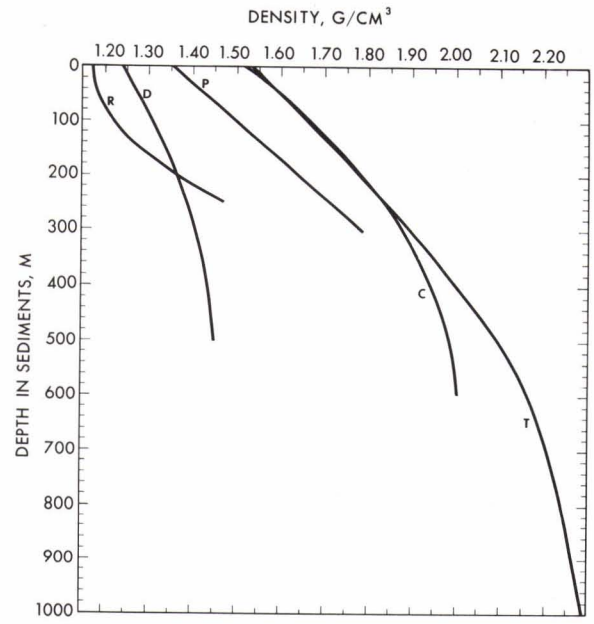

FIG. 6
IN SITU DENSITY OF VARIOUS MARINE SEDIMENTS VERSUS DEPTH IN THE SEA FLOOR. LETTERS INDICATE SEDIMENT TYPE: R IS RADIOLARIAN OOZE; D IS DIATOMACEOUS OOZE; P IS PELAGIC CLAY; C IS CALCAREOUS SEDIMENT; T IS TERRIGENOUS SEDIMENT.

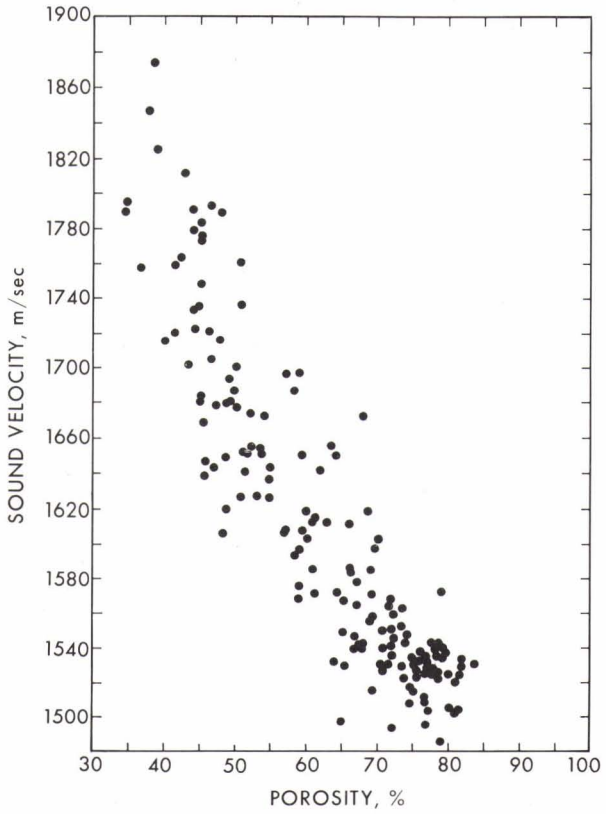

FIG. 7
SEDIMENT POROSITY VERSUS SOUND VELOCITY, CONTINENTAL TERRACE.

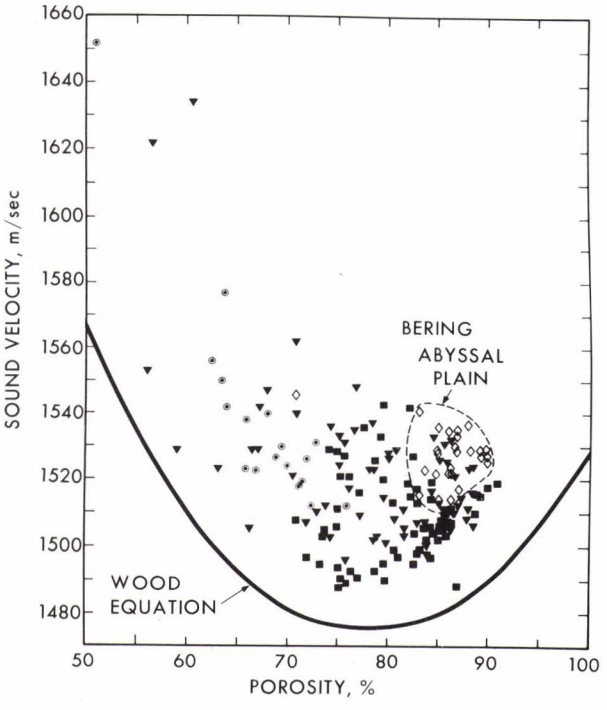

FIG. 8
SEDIMENT POROSITY VERSUS SOUND VELOCITY, ABYSSAL HILL AND ABYSSAL PLAIN ENVIRONMENTS; SYMBOLS AS IN FIGURE 2, EXCEPT CIRCLED DOTS ARE CALCAREOUS SAMPLES.

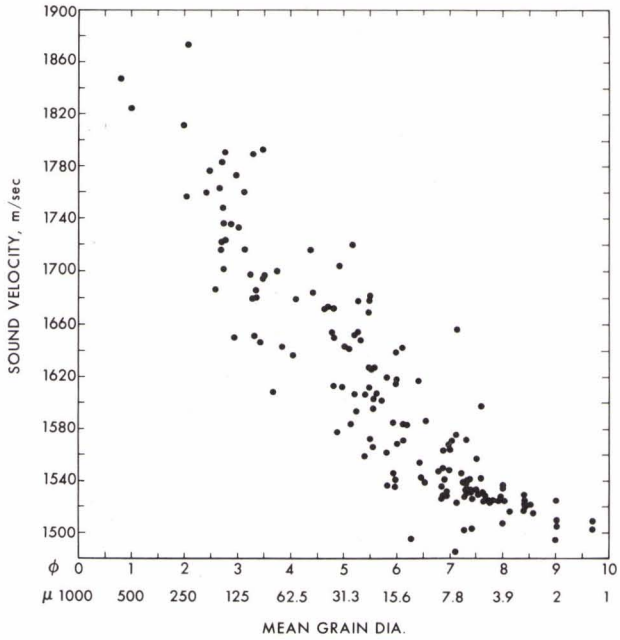

FIG. 9
MEAN DIAMETER OF MINERAL GRAINS VERSUS SOUND VELOCITY, CONTINENTAL TERRACE (SHELF AND SLOPE).

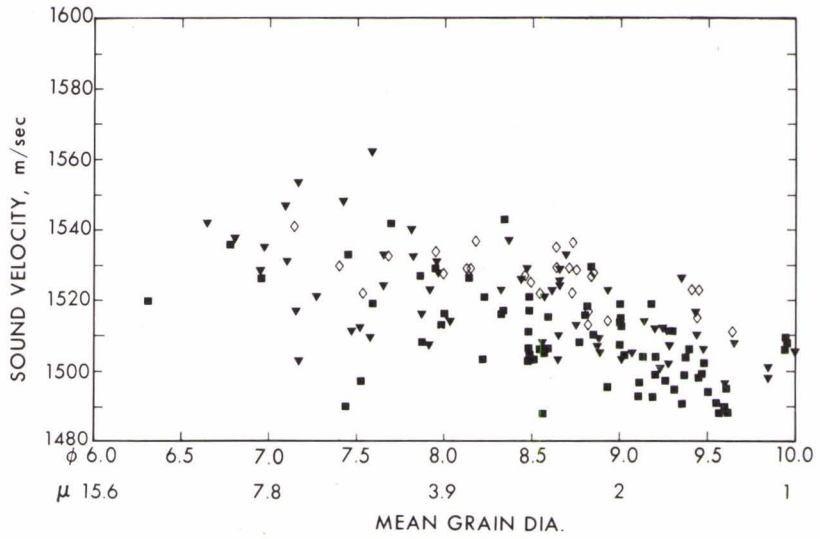

FIG. 10 MEAN DIAMETER OF MINERAL GRAINS VERSUS SOUND VELOCITY, ABYSSAL HILL AND ABYSSAL PLAIN ENVIRONMENTS; SYMBOLS AS IN FIG. 2.

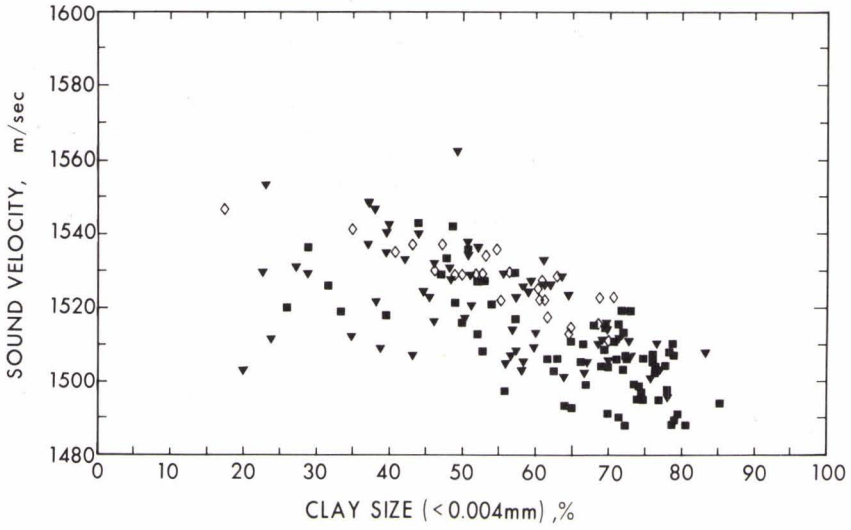

FIG. 11 PERCENT CLAY SIZE VERSUS SOUND VELOCITY, ABYSSAL HILL AND ABYSSAL PLAIN ENVIRONMENTS; SYMBOLS AS IN FIGURE 2.

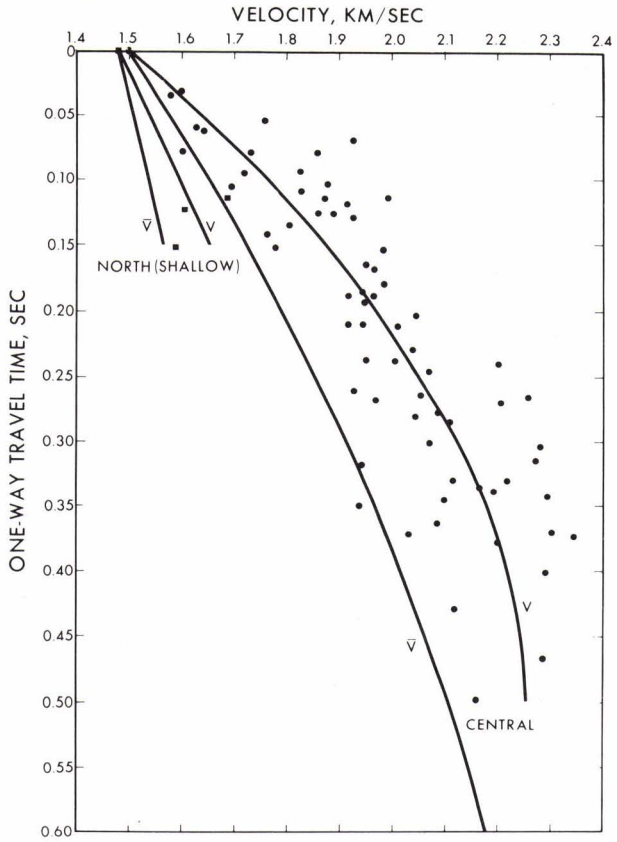

FIG. 12
INSTANTANEOUS VELOCITY, V, AND MEAN VELOCITY, $\bar{V}$, VERSUS ONE-WAY TRAVEL TIME IN THE CENTRAL (DOTS) AND NORTHERN (SQUARES) BENGAL FAN IN THE BAY OF BENGAL (FROM HAMILTON ET AL., 1974).

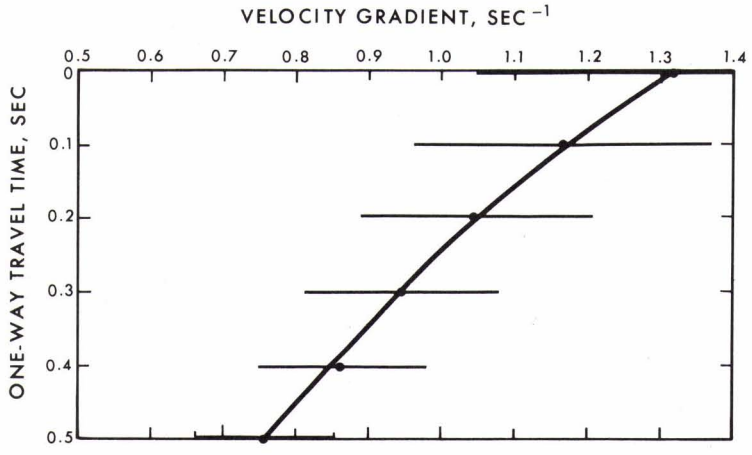

FIG. 13
AN AVERAGE LINEAR VELOCITY GRADIENT, IN METERS PER SECOND PER METER, OR SEC^{-1}, VERSUS ONE-WAY TRAVEL TIME OF SOUND IN THE SEA FLOOR. THE LINEAR GRADIENTS AT INCREMENTS OF 0.1 sec WERE AVERAGED FROM 13 AREAS IN WHICH THE SEDIMENTS WERE LARGELY TURBIDITES. THE HORIZONTAL BARS INDICATE 95 PERCENT CONFIDENCE LIMITS (REVISED FROM HAMILTON ET AL., 1974).

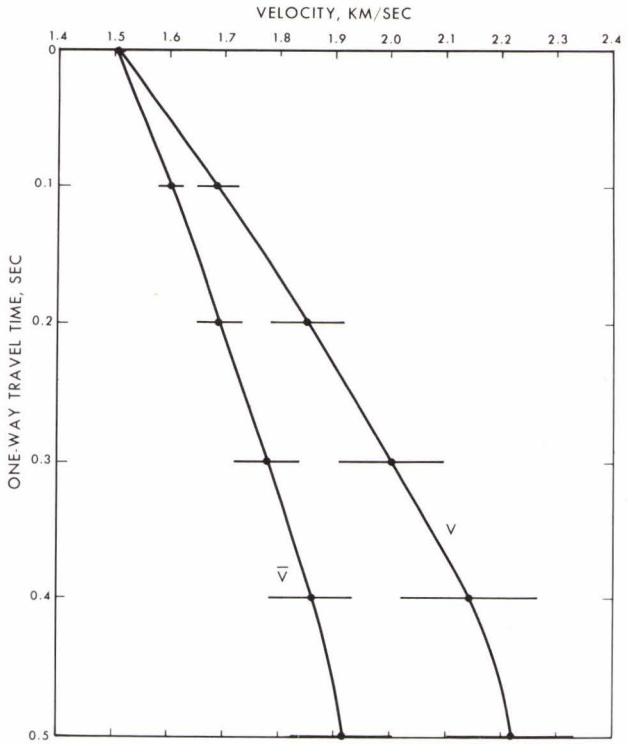

FIG. 14
INSTANTANEOUS VELOCITY, V, AND MEAN VELOCITY, $\bar{V}$, VERSUS ONE-WAY TRAVEL TIME IN THE SEA FLOOR. THE CURVES ARE AVERAGES FOR 13 AREAS IN WHICH THE SEDIMENTS ARE LARGELY TURBIDITES. THE HORIZONTAL BARS INDICATE 95 PERCENT CONFIDENCE LIMITS. SEE HAMILTON ET AL. (1974) FOR DISCUSSIONS.

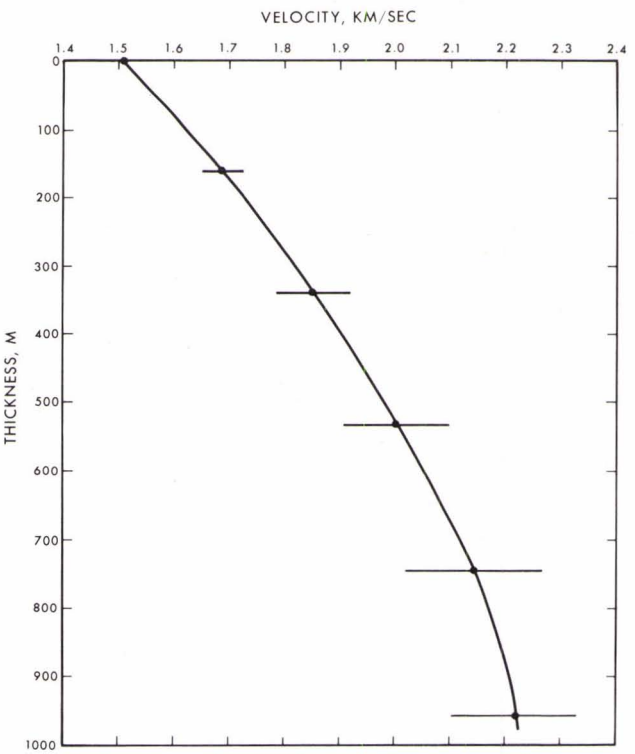

FIG. 15
INSTANTANEOUS SOUND VELOCITY VERSUS THICKNESS (OR DEPTH IN THE SEA FLOOR). THE CURVE IS AN AVERAGE FOR 13 AREAS IN WHICH THE SEDIMENTS ARE LARGELY TURBIDITES. THE HORIZONTAL BARS INDICATE 95 PERCENT CONFIDENCE LIMITS.

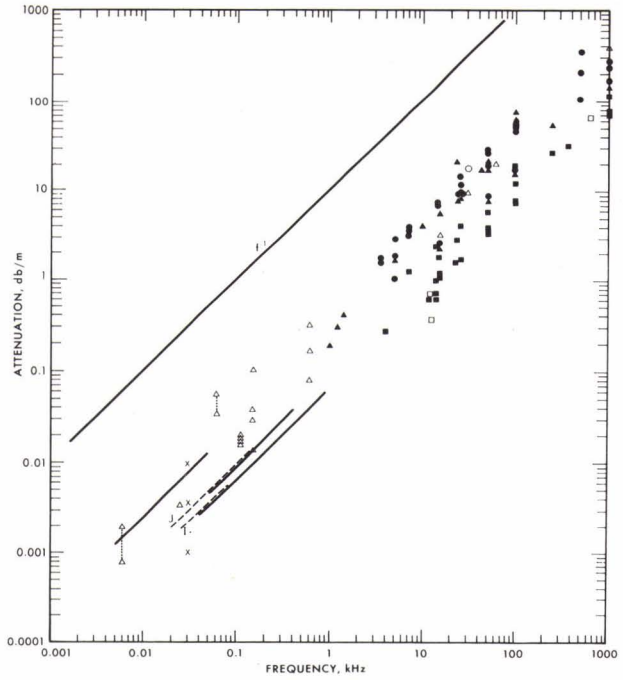

FIG. 16 ATTENUATION OF COMPRESSIONAL (SOUND) WAVES VERSUS FREQUENCY IN NATURAL, SATURATED SEDIMENTS AND SEDIMENTARY STRATA. SYMBOLS: CIRCLES–SANDS (ALL SIZES); SQUARES–CLAY–SILT (MUD); TRIANGLES– MIXED SIZES (e.g, SILTY SAND, SANDY SILT). THE SOLID LINES AND SYMBOLS ARE FROM HAMILTON (1972, Fig. 2); THE OPEN SYMBOLS AND DASHED LINES ARE NEWLY–ADDED DATA. THE LINES MARKED "J" AND "I" REPRESENT GENERAL EQUATIONS FOR THE JAPAN SEA AND INDIAN OCEAN CENTRAL BASIN (FROM NEPROCHNOV, 1971). THE VERTICAL, DASHED LINES INDICATE A RANGE OF ATTENUATION VALUES AT A SINGLE FREQUENCY. THE LINE LABELLED "f^1" INDICATES THE SLOPE OF ANY LINE HAVING A DEPENDENCE OF ATTENUATION ON THE FIRST POWER OF FREQUENCY.

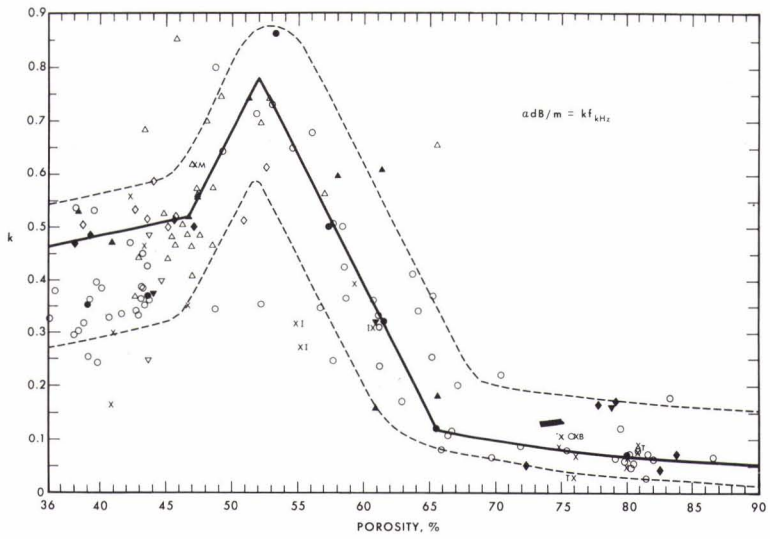

FIG. 17 ATTENUATION OF COMPRESSIONAL WAVES (EXPRESSED AS k IN: $\alpha_{dB/m} = kf_{kHz}$) VERSUS SEDIMENT POROSITY IN NATURAL, SATURATED SURFACE SEDIMENTS. SOLID SYMBOLS ARE AVERAGES AND OPEN SYMBOLS ARE THE AVERAGED DATA FROM MEASUREMENTS OFF SAN DIEGO; SOLID LINES ARE REGRESSIONS ON THE BEST DATA (See HAMILTON, 1972, for discussion); X INDICATES A VALUE FROM THE LITERATURE. THE DASHED LINES REPRESENT AREAS INTO WHICH IT IS PREDICTED MOST DATA WILL FALL. REGRESSION EQUATIONS ARE INCLUDED IN THE CAPTION TO THE ORIGINAL FIGURE (HAMILTON, 1972, Fig. 5) FOR THE SOLID LINES. NEWLY–ADDED DATA ARE THREE STATIONS IN SILTY SAND (IGARASHI, 1973) MARKED "I", AN AVERAGE OF 11 CORES OF PELAGIC CLAY (BUCHAN ET AL, 1971) MARKED "B", FINE SAND (MUIR AND ADAIR, 1972) MARKED "M", AND SILTY CLAY AND CALCAREOUS SEDIMENTS FROM TYCE (1975) MARKED "T".

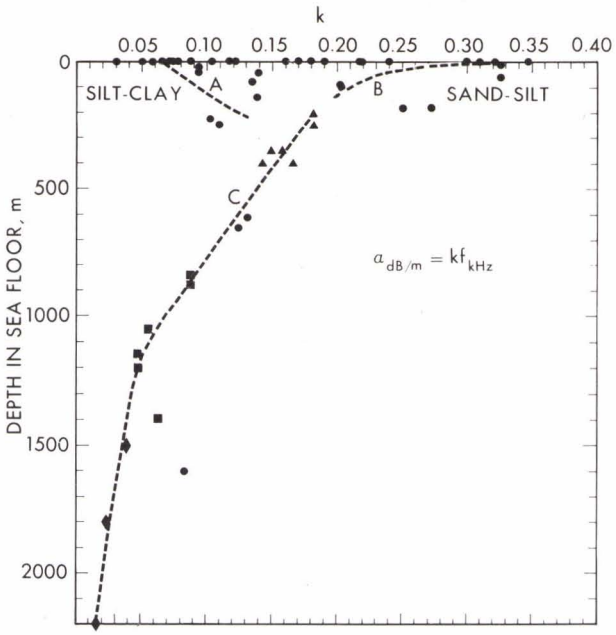

FIG. 18
ATTENUATION OF COMPRESSIONAL WAVES (EXPRESSED AS k IN : $\alpha = {}_{dB/m} = kf_{kHz}$) VERSUS DEPTH IN THE SEA FLOOR, OR IN SEDIMENTARY STRATA. SYMBOLS : CIRCLES–MEASUREMENTS FROM THE LITERATURE ; TRIANGLES, SQUARES, AND DIAMONDS REPRESENT THE FIRST, SECOND, AND THIRD LAYERS, RESPECTIVELY, IN THE SEA FLOOR IN 7 AREAS (FROM NEPROCHNOV, 1971). SEE TEXT FOR DISCUSSION OF THE LABELLED CURVES.

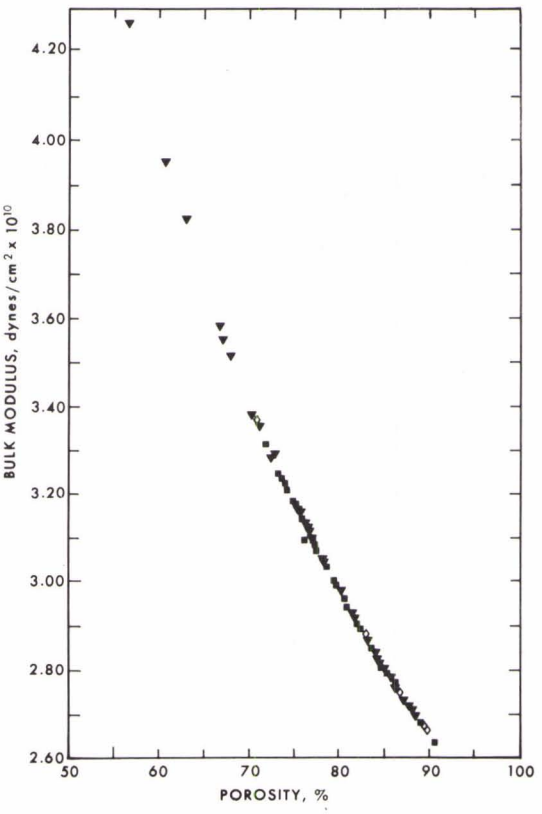

FIG. 19
SEDIMENT POROSITY VERSUS COMPUTED BULK MODULUS (23° C, 1 ATMOS.) FOR THE ABYSSAL HILL AND ABYSSAL PLAIN ENVIRONMENTS.

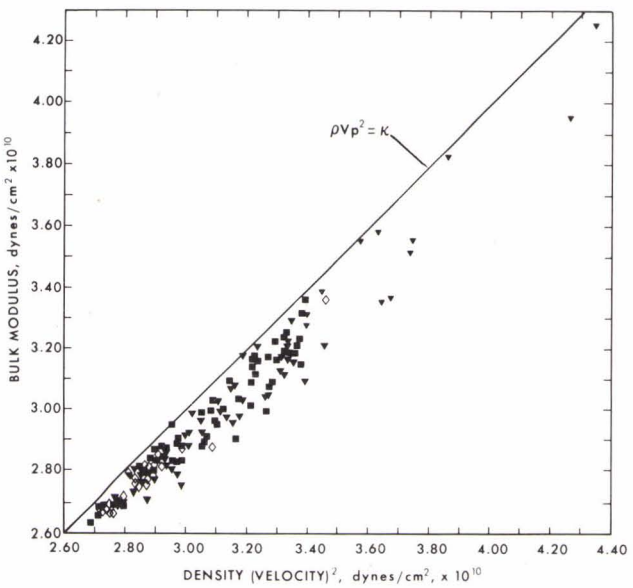

FIG. 20
DENSITY X (COMPRESSIONAL VELOCITY)^2 VERSUS COMPUTED BULK MODULUS OF SEDIMENT SAMPLES (23° C, 1 ATMOS.) IN THE ABYSSAL HILL AND ABYSSAL PLAIN ENVIRONMENTS. THE LINE LABELLED " $\rho V_p^2 = k$" INDICATES RELATIONSHIPS IF THE SAMPLES HAD NO RIGIDITY.

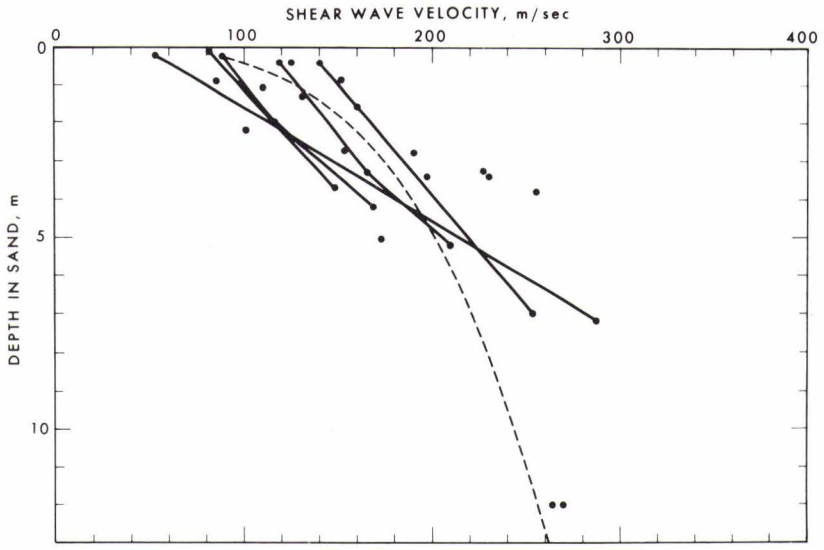

FIG. 21 SHEAR WAVE VELOCITY VERSUS DEPTH IN WATER-SATURATED SANDS. ALL MEASUREMENTS ARE IN SITU; MULTIPLE MEASUREMENTS AT THE SAME SITE ARE CONNECTED BY SOLID LINES. THE DASHED LINE IS THE REGRESSION EQUATION: $V_s = 128(D)^{0.28}$; V_s in m/sec, and D is depth in m.

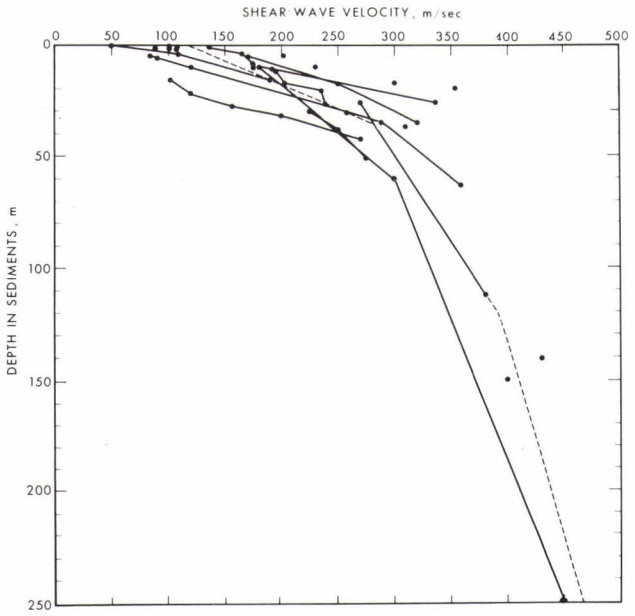

FIG. 22 SHEAR WAVE VELOCITY MEASURED IN SITU VERSUS DEPTH IN WATER-SATURATED SILT-CLAYS AND TURBIDITES. MULTIPLE MEASUREMENTS AT THE SAME SITE ARE CONNECTED BY SOLID LINES. THE DASHED LINES ARE THREE LINEAR REGRESSIONS. ONE MEASUREMENT (V_s = 700 m/sec at 650 m) IS NOT SHOWN.

TABLE 1a. Continental Terrace (Shelf and Slope) Environment; average sediment size analyses and bulk grain densities.

Sediment Type	No. Samples	Mean Grain Dia. mm	Mean Grain Dia. ϕ	Sand, %	Silt, %	Clay, %	Bulk Grain Density g/cm^3
Sand							
Coarse	2	0.5285	0.92	100.0	0.0	0.0	2.710
Fine	18	0.1638	2.61	92.4	4.2	3.4	2.708
Very fine	6	0.0915	3.45	84.2	10.1	5.7	2.693
Silty sand	14	0.0679	3.88	64.0	23.1	12.9	2.704
Sandy silt	17	0.0308	5.02	26.1	60.7	13.2	2.668
Silt	12	0.0213	5.55	6.3	80.6	13.1	2.645
Sand-silt-clay	20	0.0172	5.86	32.2	41.0	26.8	2.705
Clayey silt	60	0.0076	7.05	7.2	59.7	33.1	2.660
Silty Clay	19	0.0027	8.52	4.8	41.2	54.0	2.701

TABLE 1b. Continental Terrace (Shelf and Slope) Environment; sediment densities, porosities, sound velocities, and velocity ratios.

Sediment Type	Density, g/cm^3		Porosity, %		Velocity, m/sec		Velocity Ratio	
	Avg.	SE	Avg.	SE	Avg.	SE	Avg.	SE
Sand								
Coarse	2.034	—	38.6	—	1836	—	1.201	—
Fine	1.957	0.023	44.8	1.36	1753	11	1.147	0.007
Very fine	1.866	0.035	49.8	1.69	1697	32	1.111	0.021
Silty sand	1.806	0.026	53.8	1.60	1668	11	1.091	0.007
Sandy silt	1.787	0.044	52.5	2.44	1664	13	1.088	0.008
Silt	1.767	0.037	54.2	2.06	1623	8	1.062	0.005
Sand-silt-clay	1.590	0.026	66.8	1.46	1579	8	1.033	0.005
Clayey silt	1.488	0.016	71.6	0.87	1549	4	1.014	0.003
Silty clay	1.421	0.015	75.9	0.82	1520	3	0.994	0.002

Notes.

Laboratory values: 23° C, 1 atm; density: saturated bulk density; porosity: salt free; velocity ratio: velocity in sediment/velocity in sea water at 23° C, 1 atm, and salinity of sediment pore water. SE: Standard error of the mean.

TABLE 2a. Abyssal Plain and Abyssal Hill Environments; average sediment size analyses and bulk grain densities.

Environment Sediment Type	No. Samples	Mean Grain Dia. mm	Mean Grain Dia. ϕ	Sand, %	Silt, %	Clay, %	Bulk Grain Density, g/cm^3
Abyssal Plain							
Sandy silt	1	0.0170	5.88	19.4	65.0	15.6	2.461
Silt	3	0.0092	6.77	3.2	78.0	18.8	2.606
Sand-silt-clay	2	0.0208	5.59	35.2	33.3	31.5	2.653
Clayey silt	22	0.0053	7.57	4.5	55.3	40.2	2.650
Silty clay	40	0.0021	8.90	2.5	36.0	61.5	2.660
Clay	6	0.0014	9.53	0.0	22.2	77.8	2.663
Bering Sea and Okhotsk Sea (Diatomaceous)							
Silt	1	0.0179	5.80	6.5	76.3	17.2	2.474
Clayey silt	5	0.0049	7.68	8.1	49.1	42.8	2.466
Silty clay	23	0.0024	8.71	3.0	37.4	59.6	2.454
Abyssal Hill							
Deep-sea ("red") pelagic clay							
Clayey silt	17	0.0056	7.49	3.9	58.7	37.4	2.678
Silty clay	60	0.0023	8.76	2.1	32.2	65.7	2.717
Clay	45	0.0015	9.43	0.1	19.0	80.9	2.781
Calcareous ooze							
Sand-silt-clay	5	0.0146	6.10	27.3	42.8	29.9	2.609
Silt	1	0.0169	5.89	16.3	75.6	8.1	2.625
Clayey silt	15	0.0069	7.17	3.4	60.7	35.9	2.678
Silty clay	4	0.0056	7.48	3.9	39.9	56.2	2.683

TABLE 2b. Abyssal Plain and Abyssal Hill Environments; sediment densities, porosities, sound velocities, and velocity ratios.

Environment Sediment Type	Density, g/cm^3		Porosity, %		Velocity, m/sec		Velocity Ratio	
	Avg.	SE	Avg.	SE	Avg.	SE	Avg.	SE
Abyssal Plain								
Sandy silt	1.652	—	56.6	—	1622	—	1.061	—
Silt	1.604	—	63.6	—	1563	—	1.022	—
Sand-silt-clay	1.564	—	66.9	—	1536	—	1.004	—
Clayey silt	1.437	0.023	75.2	1.31	1526	3	0.998	0.002
Silty clay	1.333	0.019	81.4	1.03	1515	2	0.991	0.001
Clay	1.352	0.037	80.0	2.20	1503	2	0.983	0.001
Bering Sea and Okhotsk Sea (Diatomaceous)								
Silt	1.447	—	70.8	—	1546	—	1.011	—
Clayey silt	1.228	0.019	85.8	0.86	1534	2	1.003	0.001
Silty clay	1.214	0.008	86.8	0.43	1525	2	0.997	0.001
Abyssal Hill								
Deep-sea ("red") pelagic clay								
Clayey silt	1.347	0.020	81.3	0.95	1522	3	0.995	0.002
Silty clay	1.344	0.011	81.2	0.60	1508	2	0.986	0.001
Clay	1.414	0.012	77.7	0.64	1493	1	0.976	0.001
Calcareous ooze								
Sand-silt-clay	1.400	0.013	76.3	0.90	1581	8	1.034	0.005
Silt	1.725	—	56.2	—	1565	—	1.023	—
Clayey silt	1.573	0.020	66.8	1.22	1537	5	1.005	0.003
Silty clay	1.483	0.029	72.3	1.61	1524	7	0.996	0.005

Notes:

Laboratory values: 23° C, 1 atm; density: saturated bulk density; porosity: salt free; velocity ratio: velocity in sediment/velocity in sea water at 23° C, 1 atm, and salinity of sediment pore water. SE: Standard error of the mean.

TABLE 3. Continental Terrace (Shelf and Slope) Environment; average sediment impedances, density (velocity)^2, reflection coefficients, and bottom losses.

Sediment Type	$\rho_2 V_2$	$\rho_2 (V_2)^2$	R	BL
Sand				
Coarse	3.7344	6.8564	0.4098	7.7
Fine	3.4302	6.0125	0.3739	8.5
Very fine	3.1662	5.3725	0.3389	9.4
Silty sand	3.0129	5.0265	0.3168	10.0
Sandy silt	2.9732	4.9468	0.3108	10.1
Silt	2.8675	4.6534	0.2944	10.6
Sand-silt-clay	2.5106	3.9643	0.2326	12.7
Clayey silt	2.3049	3.5703	0.1917	14.3
Silty clay	2.1596	3.2822	0.1602	15.9

Notes.

Laboratory values: 23°C, 1 atmosphere.

$\rho_2 V_2$ = sediment impedance, g/cm^{2}sec x 10^5.

$\rho_2 (V_2)^2$ = sediment density X (velocity)^2, g/cmsec^2, or dynes/cm^2, x 10^{10}.

R = Rayleigh reflection coefficient at normal incidence = $\dfrac{\rho_2 V_2 - \rho_1 V_1}{\rho_2 V_2 + \rho_1 V_1}$

BL = -20 log R, bottom loss, dB.

ρ_1, V_1: sea-water density, velocity; ρ_2, V_2: sediment density, velocity.

TABLE 4. Abyssal Plain and Abyssal Hill Environments; average sediment impedances, density (velocity)^2, reflection coefficients, and bottom losses.*

Environment Sediment Type	$\rho_2 V_2$	$\rho_2 (V_2)^2$	R	BL
Abyssal Plain				
Sandy silt	2.6795	4.3462	0.2623	11.6
Silt	2.5071	3.9185	0.2311	12.7
Sand-silt-clay	2.4023	3.6899	0.2107	13.5
Clayey silt	2.1929	3.3463	0.1668	15.6
Silty clay	2.0195	3.0594	0.1265	18.0
Clay	2.0321	3.0542	0.1295	17.8
Bering Sea and Okhotsk Sea (Diatomaceous)				
Silt	2.2371	3.4585	0.1763	15.1
Clayey silt	1.8840	2.8904	0.0920	20.7
Silty clay	1.8514	2.8233	0.0833	21.6
Abyssal Hill				
Deep-sea ("red") pelagic clay				
Clayey silt	2.0501	3.1203	0.1339	17.5
Silty clay	2.0268	3.0563	0.1283	17.8
Clay	2.1111	3.1519	0.1482	16.6
Calcareous ooze				
Sand-silt-clay	2.2137	3.5003	0.1714	15.3
Silt	2.6996	4.2249	0.2658	11.5
Clayey silt	2.4175	3.7155	0.2138	13.4
Silty clay	2.2598	3.4435	0.1813	14.8

* See notes under Table 3.

TABLE 5. Continental Terrace (Shelf and Slope) Environment; computed elastic constants in sediments.

Sediment Type	κ Avg.	κ SE	σ Avg.	σ SE	μ Avg.	μ SE	V_s Avg.	V_s SE	No. Samples
Sand									
Coarse	6.6859	—	0.491	—	0.1289	—	250	—	2
Fine	5.5063	0.1638	0.466	0.005	0.3713	0.0509	417	37	15
Very fine	5.0243	0.3479	0.456	0.010	0.4501	0.1228	472	62	5
Silty sand	4.5017	0.1327	0.459	0.006	0.3716	0.0452	447	27	13
Sandy silt	4.4487	0.2137	0.469	0.007	0.2745	0.0613	363	47	13
Silt	4.3320	0.1631	0.484	0.003	0.1324	0.0187	270	27	9
Sand-silt-clay	3.5903	0.0907	0.463	0.003	0.2784	0.0223	412	17	18
Clayey silt	3.3173	0.0450	0.476	0.002	0.1687	0.0135	324	12	50
Silty clay	3.1459	0.0353	0.484	0.002	0.1026	0.0101	263	12	19

Notes.

Laboratory values: 23°C, 1 atmosphere pressure.

κ = bulk modulus, dynes/cm^2 x 10^{10}.

μ = rigidity (shear) modulus, dynes/cm^2 x 10^{10}.

σ = Poisson's Ratio.

V_s = velocity of shear wave, m/sec.

SE= Standard error of the mean. Data through 1973 in this table.

TABLE 6. Abyssal Plain and Abyssal Hill Environments; computed elastic constants in sediments.*

Environment / Sediment Type	κ Avg.	κ SE	σ Avg.	σ SE	μ Avg.	μ SE	V_s Avg.	V_s SE	No. Samples
Abyssal Plain									
Sandy silt	4.2572	—	0.492	—	0.0668	—	201	—	1
Silt	3.5798	—	0.484	—	0.1291	—	254	—	2
Sand-silt-clay	3.5670	—	0.488	—	0.0898	—	228	—	2
Clayey silt	3.1465	0.0479	0.480	0.002	0.1286	0.0126	292	16	21
Silty clay	2.8963	0.0391	0.487	0.001	0.0798	0.0078	238	11	34
Clay	3.0108	0.1048	0.493	0.001	0.0421	0.0079	173	20	5
Bering Sea and Okhotsk Sea (Diatomaceous)									
Silt	3.3610	—	0.489	—	0.0731	—	225	—	1
Clayey silt	2.7969	0.0222	0.488	0.004	0.0711	0.0247	224	41	5
Silty clay	2.7381	0.0191	0.488	0.002	0.0648	0.0079	225	12	22
Abyssal Hill									
Deep-sea ("red") pelagic clay									
Clayey silt	2.9955	0.0625	0.481	0.003	0.1165	0.0170	287	21	8
Silty clay	2.9455	0.0267	0.487	0.001	0.0759	0.0060	229	9	48
Clay	2.9474	0.0467	0.491	0.001	0.0512	0.0038	194	7	14
Calcareous ooze									
Sand-silt-clay	3.1370	0.0381	0.458	0.005	0.2730	0.0280	439	24	5
Clayey silt	3.5587	0.0529	0.488	0.001	0.0877	0.0077	234	10	14
Silty clay	3.3139	0.0779	0.485	0.002	0.0978	0.0137	255	17	4

* See notes under Table 5. Data through 1973 in this table

APPENDIX A: EQUATIONS FOR REGRESSION LINES AND CURVES

Regression lines and curves were computed for those illustrated sets of (x,y) data that constitute the best indices (x) to obtain desired properties (y). Separate equations are listed, where appropriate, for each of the three general evvironments, as follows: continental terrace (shelf and slope), (T); abyssal hill(pelagic), (H); abyssal plain (turbidite), (P). The equations are keyed by figure numbers to the related scatter diagrams in the main text. The Standard Errors of Estimate, σ, opposite each equation, are applicable only near the mean of the (x, y) values, and accuracy of the (y) values, given (x), falls off away from this region (Griffiths, 1967,p. 448). Grain sizes are shown in the logarithmic phi-scale ($\phi = -\log_2$ of grain diameter in millimeters).

It is important that the regression equations be used only between the limiting values of the index property (x values), as noted below. These equations are strictly empirical and apply only to the (x,y) data points involved. There was no attempt, for example, to force the curves expressed by the equations to pass through velocity values of minerals at zero porosity, or the velocity value of sea water at 100 percent porosity.

The limiting values of (x), in the equations below, are:

(1) Mean grain diameter, M_z,ϕ

(T) 1 to 9 ϕ

(H) and (P) 7 to 10 ϕ

(2) Porosity, n, percent

(T) 35 to 85 percent

(H) and (P) 70 to 90 percent

(3) Density, ρ, g/cm^3

(T) 1.25 to 2.10 g/cm^3

(H) 1.15 to 1.50 g/cm^3

(P) 1.15 to 1.70 g/cm^3

(4) Clay size grains, C, percent

(H) and (p) 20 to 85 percent

(5) Density × (Velocity)^2, ρV_p^2, dynes $/cm^2 \times 10^{10}$

(H) 2.7 to 3.4 dynes/$cm^2 \times 10^{10}$

(P) 2.7 to 3.8 dynes/$cm^2 \times 10^{10}$

Porosity, n (%) vs. Mean Grain Diameter, M_z (ϕ) Figure 3

(T) $n = 30.95 + 5.50(M_z)$ $\sigma = 6.8$

(H) $n = 82.42 - 0.29(M_z)$ $\sigma = 4.7$

(P) $n = 45.43 + 3.93(M_z)$ $\sigma = 6.5$

Density, p (g/cm^3) vs. Mean Grain Diameter, M_z (ϕ) Figure 2

(T) $p = 2.191 - 0.095(M_z)$ $\sigma = 0.12$

(H) $p = 1.327 + 0.005(M_z)$ $\sigma = 0.09$

(P) $p = 1.879 - 0.06(M_z)$ $\sigma = 0.11$

Sound Velocity, V_p (m/sec) vs. Mean Grain Diameter, M_z (ϕ) Figures 9,10

(T) $V_p = 1924.9 - 74.18(M_z) + 3.04(M_z)^2$ $\sigma = 33.6$

(H) $V_p = 1594.4 - 10.2(M_z)$ $\sigma = 11.6$

(P) $V_p = 1631.8 - 13.3(M_z)$ $\sigma = 18.3$

Sound Velocity, V_p (m/sec) vs. Porosity, n (%) Figures 7,8

(T) $V_p = 2467.3 - 22.13(n) + 0.129(n)^2$ $\sigma = 33.7$

(H) $V_p = 1410.8 + 1.175(n)$ $\sigma = 13.3$

(P) $V_p = 1630.8 - 1.402(n)$ $\sigma = 20.6$

Sound Velocity, V_p (m/sec) vs. Density, ρ (g/cm^3)

(T) $V_p = 2263.0 - 1164.8(\rho) + 458.8(\rho)^2$ $\sigma = 34.2$

(H) $V_p = 1591.7 - 63.5(\rho)$ $\sigma = 13.2$

(P) $V_p = 1430.6 + 65.2(\rho)$ $\sigma = 21.7$

Sound Velocity, V_p (m/sec) vs. Clay Size, C (%) Figure 11

(H) $V_p = 1549.4 - 0.66(C)$ $\sigma = 9.9$

(P) $V_p = 1568.8 - 0.89(C)$ $\sigma = 18.3$

Density, ρ (g/cm^3) vs. Porosity, n (%)

(T) $n = 156.0 - 56.8(\rho)$ $\sigma = 2.7$

(H) $n = 150.1 - 51.2(\rho)$ $\sigma = 1.2$

(P) $n = 159.6 - 58.9(\rho)$ $\sigma = 1.4$

Bulk Modulus, K (dynes/cm^2 $\times$ 10^{10}) vs. Porosity, n (%) Figures 19

(T) $K = 215.09467 - 133.1006\ (\log_e n) + 28.2872\ (\log_e n)^2 - 2.0446\ (\log_e n)^3$ $\sigma = 0.01146$

(H) and (P) $K = 128.9909 - 72.0478\ (\log_e n) + 13.8657\ (\log_e n)^2 - 0.9097\ (\log_e n)^3$ $\sigma = 0.0100$

Bulk Modulus, κ (dynes/cm^2 $\times$ 10^{10}) vs.

Density $\times$ (velocity)^2, ρV_p^2 (dynes/cm $\times$ 10^{10})

(H) $\kappa = 0.32039 + 0.862\ (\rho V_p^2)$ $\sigma = 0.049$

(P) $\kappa = 1.68823 + 0.134\ (\rho V_p^2)$ $\sigma = 0.069$

Note: The figures (numbers noted above) are from Hamilton (1974a). The regression equations include all new measurements to July 1975; these new data would not add significantly to the scatter diagrams.

APPENDIX B: CONTRUCTION OF GEOACOUSTIC MODELS

The acoustic properties of the sea floor for specific areas must be compiled into quantitative geoacoustic models to be of use to the acoustician. In 1973, the writer summarized and illustrated the methods used at the Naval Undersea Center to construct these models (Hamilton, 1974b). For the convenience of the reader, this information is reproduced in this Appendix. It should be noted that additional information can be supplied in those categories studied since 1973 (and, as yet, unpublished), and briefly discussed in appropriate sections of this report; namely: the profiles and gradients of density, porosity, and compressional wave attenuation with depth in the sea floor, and a suggested method for approximating the attenuation of shear waves.

DATA REQUIRED TO CONSTRUCT GEOACOUSTIC MODELS

Introduction

The real sea floor cannot be defined by any single geoacoustic model; therefore, it is important that acoustic and geophysical experiments at sea involving the sea floor be supported by a particular model of the area. However, it is possible to use geologic and geophysical judgment to extrapolate a general model over wider areas. A sufficient collection of models from diverse environments will allow predictions of bottom models in similar areas of the world's oceans.

A geoacoustic model should detail the real sea floor. It can then be used in studies of reflection and refraction of compressional and shear waves over a wide range of frequencies, in geologic studies of stratigraphy, sedimentology, and geologic history, and in various other studies in the field of geophysics (e.g., gravity computations).

The production of a geoacoustic model of the sea floor requires assembly of data from a wide variety of sources in the fields of oceanography, geology, and geophysics. A model thus brings into focus and utility, data from many scientific disciplines and operations at sea and in the laboratory. The gross layering may be all that is required in some geologic and geophysical studies, but the acoustician must be supplied sufficient detail to study insonified areas at various sound frequencies.

Data Required and Methods

In an ideal production of a geoacoustic model, the following data should be derived at sea and in the laboratory. In addition, associated information from all available sources, published and unpublished, should be sought and selectively used.

Data for a bathymetric chart. The first requisite of a geoacoustic model is a good bathymetric chart of the insonified (and adjacent) area. Data required includes: (1) all available sounding data from government sources and oceanographic institutions (published and unpublished), (2) a careful record of all ship's movements on station, (3) continuous echo sounding records, (4) a Nansen cast or other data which allows corrections from echo-sounder to true depths, (5) location by satellite navigation methods. In the laboratory, the smoothed ship's track is plotted with soundings, and all available data is used to produce a good contoured chart of the insonified and adjacent areas. It can rarely be assumed that any given, published chart of an area is valid. Very little of the sea floor has been charted properly, in detail.

Data to determine layer thicknesses and locations of reflectors. Continuous seismic reflection profiling determines travel time between impedance mismatches, or reflectors. Air-gun power sources can obtain data at low frequencies on the order of 20 to 50 Hz. Electric 'sparker' sources usually are operated between about 80 and 250 Hz. Layering

can be seen at 12 kHz by the normal echo sounder operating on a short ping to depths in silt-clay sediments on the order of 5 to 20 m. The 3.5 kHz system frequently shows reflectors in silt-clays to depths of 40 to 60 m.

Given travel time in a sediment layer, the true thickness can be derived if the interval velocity, or velocity gradient is known. At present, these data are usually acquired from wide-angle reflection measurements using expendable sonobuoys (LePichon et al., 1968; Houtz et al.,1968).

Water-Mass data. To predict in situ sediment surface properties, it is necessary to have information on the sound velocity, density, and salinity of the sea water at the water-sediment interface. These data can be derived from a normal Nansen cast; a curve showing sound velocity vs. water depth is particularly useful.

Data on sea-floor relief. Details of bottom topography, roughness, relief, and slope are required for some acoustic studies. These can be determined by surface echo sounders (especially those with narrow beams), underwater cameras, and deep-towed equipment.

Data on rock layers. Rock layers at or near the sea floor are important to the underwater acoustician or geophysicist. At low frequencies, all of the sediment column, and deeply buried rock layers can be important. Information is required on, at least, the density, compressional-wave velocity, and attenuation in these rock layers.

Data for sediment properties. Sediment samples from gravity and piston corers, box corers, or other samplers is required to obtain sediment physical properties. Sound velocities can be measured aboard ship, or the samples can be preserved under sea water in the refrigerator for velocity and other laboratory measurements.

In the laboratory, the minimum physical property measurements should include grain size analyses (mean grain size, and percentages of sand, silt, and clay), bulk grain density, saturated density, porosity, and additional sound velocity measurements. Other properties can be computed or predicted through these measured properties.

In shallow water, the best data can be obtained by in situ measurements for some properties (e.g., as in Hamilton et al.,1970; Hamilton, 1972).

If all of the above data are not available, or if there is no data at all, certain in situ predictions can be made following Hamilton (1971b). Predictions of layer thicknesses and attenuation (not included in the 1971 report) will be briefly noted below.

COMMON GEOACOUSTIC MODELS

Among an almost infinite variety of geoacoustic models there are four very common ones. Two of these are in the continental shelf and two in deep-sea areas. Actual gross models will illustrate these types.

Shallow-Water Geoacoustic Models

A common stratigraphy in continental shelves is a top layer of soft mud, or clay-silts, overlying harder silts and sands. This is common because during lowered sea levels of the Pleistocene, sand was deposited over wide areas of the shelf, and then covered with silt-clays as sea level rose. Figure B.1, from an actual station on the shallow Asiatic continental shelf, illustrates this model.

The other common shallow-water model is a layer of thick sand, usually overlying rock (Figure B.2). The sand usually forms a high-density, high-velocity (hence high-impedance) layer in which sound attenuation is also high. Subbottom layers are not usually acoustically seen in these areas.

Deep-Sea Geoacoustic Models

In the deep-sea there are two common models: one in abyssal plains and one in abyssal hills.

In abyssal hills, there is usually a single layer of pelagic silt-clays, with or without volcanic ash layers, over volcanic or sedimentary rock. The sediment layer may be quite thin as demonstrated in the Pacific by the Deep Sea Drilling Project, and by reflection surveys (e.g., Ewing et al., 1968). This type of geoacoustic model is illustrated in Figure B.3. The general area is the north central Pacific, west of the Aleutian Abyssal Plain. The area is in the volcanic ash zone as described by Horn et al. (1969).

As previously noted, when sedimentary layers are thin, or when frequencies are very low, the model must include properties of the rock layers. Much of the Pacific has a silt-clay layer (overlying basalt) in which one-way sound travel time is 0.05 sec or less (Ewing et al., 1968); these layers will usually be 50 to 100 m thick.

Rock velocities can usually be obtained from refraction surveys in or near the area of interest. For example, in the area represented by Figure B.3, the rock is basalt as determined by the Deep Sea Drilling Project, and an average velocity in the top of the basalt is 5.7 km/sec (Houtz et al., 1970). Given a rock velocity, the best procedure to get density, at present, is to enter diagrams relating density and velocity (e.g., Nafe and Drake, 1967; Christensen and Salisbury, 1975; Dortman and Magid, 1969). Approximate attenuation values for different rock types can usually be derived from the literature (e.g., Balakrishna and Ramana, 1968; Levykin, 1965).

The less common deep-sea geoacoustic model is from abyssal plains where turbidity currents have laid down alternating sequences of silt-clays and silt-sands (turbidites). These sediments over rock can vary in thickness from a few meters to over 2000 m. The section might comprise hundreds of layers. Most of these layers have been deposited by flows which top the natural levees of great undersea channels, and individual layers vary in thickness and cannot usually be correlated over appreciable distances. Only a few of these

layers are usually cored, and some deeper layers are seen as reflectors by echo sounders and reflection equipment. For the acoustician who requires a fully-layered model, the geologist-geophysicist should detail the layering (reflectors) as deep as he can from cores and reflection records, and then accept an alternation of probable 'average layers' to the full thickness of the sediment layer.

Figure B.4 represents the deep-water turbidite model; it is from the southern Japan Sea Abyssal Plain. The total thickness of the turbidite layer was determined by reflection profiling (to get sound-travel time in the sediment layer), and an interval velocity measurement using the sonobuoy technique developed at Lamont-Doherty Geological Observatory by Houtz and his colleagues (Houtz et al., 1968; Le Pichon et al., 1968). In the inset is a diagram from the 12 kHz echo sounder which shows detailed layering to about 10 meters. The first line (at 0 m) is the sea floor. About one m below the sea floor is a strong reflector. The corer dropped through a silty clay layer and stopped in a sand layer. Measurements in the cored sediment indicated that the first meter had a velocity a little more than one percent less than velocity in the bottom water. In situ layer velocities and densities were: first layer, 1467 m/sec and 1.23 g/cm^3; second layer, 1819 m/sec and 2.02 g/cm^3. The linear velocity gradient is from the sediment-surface velocity through the sonobuoy interval velocity.

DETAILED GEOACOUSTIC MODEL

General

The large, gross models illustrated and discussed above are of interest and utility, but for most studies of reflection and bottom loss, it has been determined that a fully-layered model must be used to reconcile experiment with theory; recent examples of this are in reports by Hastrup (1970) in the Mediterranean, and by Morris (1970) in the Pacific. For the acoustician who needs fully-layered models, all available data, estimates, and predictions are used to indicate probable layering and sediment properties down to and including the 'acoustic basement' (usually sedimentary or volcanic rock). In these estimates, available data from other sources are used: the general geologic and geophysical literature, Navy reports, unpublished data, data on similar sediments, and a certain amount of geologic 'intuition and judgment.'

At the Naval Undersea Center, our models include a gross figure such as described, plus a topographic chart of the area of the experiment, and slope and relief as seen by the echo sounder and lowered camera. The acoustician requires quantitative information. He should not have to try to measure it off figures or curves. Consequently, each model is accompanied by 5 tables and a general information sheet.

In the following section, the various tables and their headings are explained. The subsections are keyed by number to the tables, and explain the headings in each table with some explanatory discussion. The numbers in the tables are

examples and are part of the model represented by Figure B.3. Values not in parentheses were measured. The subject of predictive methods and corrections from laboratory to in situ properties was discussed in a recent report (Hamilton, 1971b).

A general information form sheet is furnished for each station; it accompanies the 5 tables. The general information sheet includes station location (Lat., Long.), maximum and minimum water depths in fathoms and meters (both echo-sounder and corrected depths), the general geographic area (e.g., the north-central Pacific), the geomorphic province (e.g., abyssal hills), and a brief description of the sea floor (topography, sediment distributions, stratigraphy, structure).

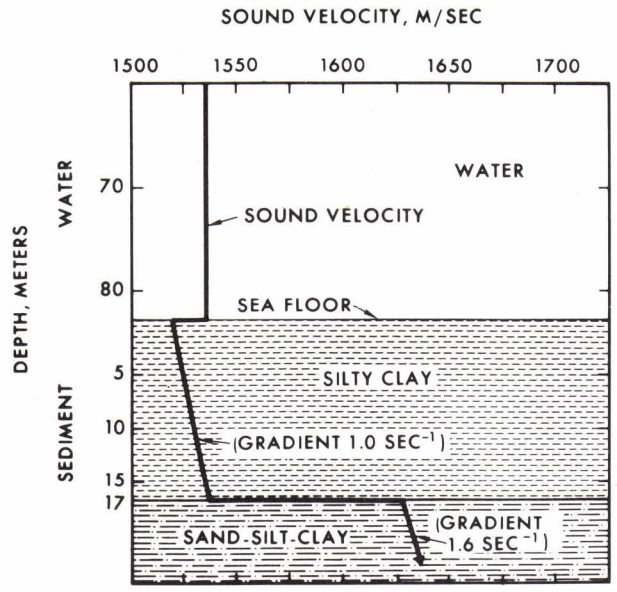

FIG. B.1 ONE OF TWO COMMON SHALLOW-WATER GEOACOUSTIC MODELS: MUD OVER SAND OR ROCK (SANDY SEDIMENTS IN THIS CASE). THE VELOCITY GRADIENT IS ASSUMED.

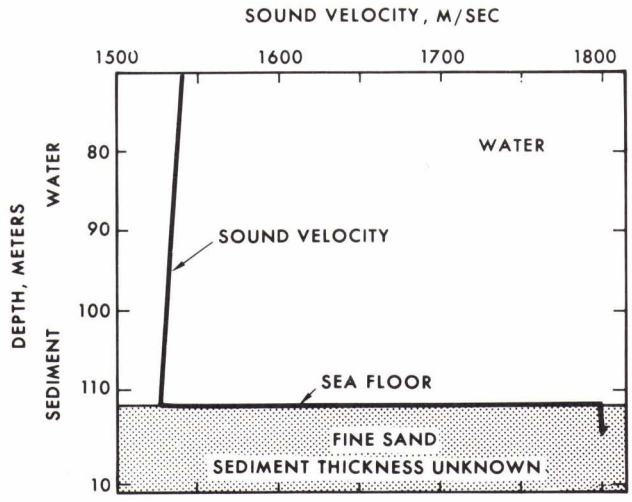

FIG. B.2 ONE OF TWO COMMON SHALLOW-WATER GEOACOUSTIC MODELS : A THICK LAYER OF HIGH-DENSITY, HIGH-VELOCITY SAND OVER ROCK. THE SLOPE OF THE GRADIENT LINE IN THE SAND HAS NO SIGNIFICANCE. SOUND VELOCITY IN SANDS INCREASES WITH ABOUT THE 0.015 POWER OF DEPTH.

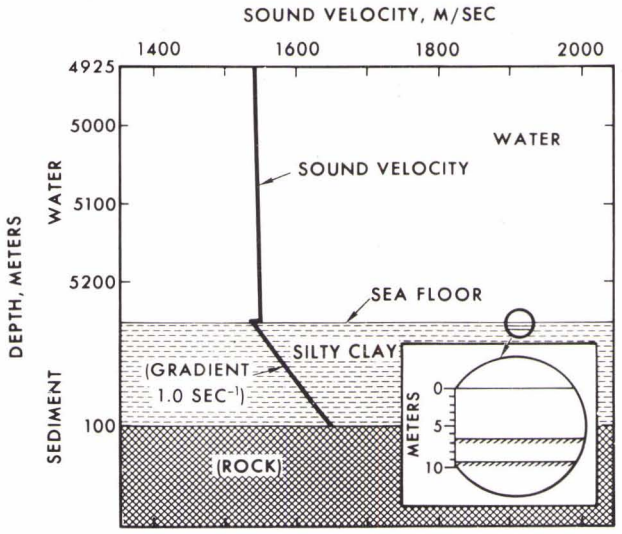

FIG. B.3 ONE OF TWO COMMON DEEP-SEA GEOACOUSTIC MODELS (ABYSSAL HILLS). THIS MODEL FROM THE NORTH PACIFIC ABYSSAL HILLS, REPRESENTS A THIN (100 m) LAYER OF PELAGIC DEEP-SEA CLAY OVERLYING BASALT. THE INSET FIGURE SHOWS REFLECTORS (AS SEEN ON 12 kHz RECORDS) WHICH ARE PROBABLY FORMED BY VOLCANIC ASH. APPENDIX B HAS FIVE TABLES WHICH ACCOMPANY THIS FIGURE, AND GIVE NUMERICAL DETAILS WHICH ARE DISCUSSED IN THE TEXT IN APPENDIX B.

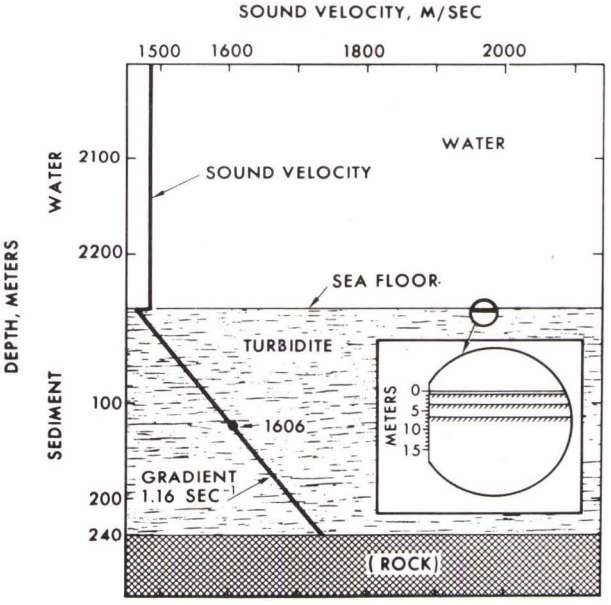

FIG. B.4 ONE OF TWO COMMON DEEP-WATER GEOACOUSTIC MODELS (ABYSSAL PLAINS). THIS MODEL, FROM THE JAPAN SEA ABYSSAL PLAIN, REPRESENT 240 m OF MULTI-LAYERED TURBIDITES OVERLYING ROCK. THE INTERVAL VELOCITY (1606 m/sec) WAS MEASURED BY THE SONOBUOY TECHNIQUE. THE LINEAR GRADIENT IS FROM THE SEDIMENT SURFACE VELOCITY (AS MEASURED IN A CORE AND CORRECTED TO IN SITU) THROUGH THE INTERVAL VELOCITY. THE INSET FIGURE SHOWS REFLECTORS AS SEEN IN 12 kHz RECORDS. A CORE IN THE AREA SHOWED THAT THE FIRST LAYER (ABOUT 1 m THICK) WAS SILTY CLAY AND THE SECOND LAYER (A STRONG REFLECTOR) WAS SAND.

Table B.1 In Situ Properties of Bottom Water

TRUE DEPTH was determined by correcting the echo-sounder depth to true depth. This additive correction is based on the velocity profile in the water mass derived from station Nansen casts. A small table supplied by the Acoustic Propagation Division, (Code 503, at NUC), is inset in the bathymetric chart (fig. 1 for each station) to indicate the value of these corrections and to permit correction of the echo-sounder depths on the contour charts to true depths. Such corrections can also be obtained from NAVOCEANO (1966).

TEMPERATURE, SALINITY, PRESSURE, and SOUND SPEED were derived from Nansen-cast data at the indicated true depth.

IMPEDANCE was computed by the formula: density x sound speed.

Table B.2 In Situ Physical Properties of Sediments (Other Than Acoustic)

The THICKNESSES of sediment layers were determined from cores, 12-kHz, and 3.5-kHz echo-sounder records, acoustic reflections (sparker), sonobuoys, and probabilities of layering (determined in similar sediments or taken from reports of other institutions for the area).

Below coring depths in the sediment, thicknesses of relatively thin layers between reflectors can be computed by measuring sound travel time between reflectors from an echo sounder record (12 or 3.5 kHz) and multiplying by a velocity extrapolated from layers above (using a velocity gradient, as

discussed in the main text). The true thicknesses of the reflecting layers (reflectors) can be estimated from the thicknesses of cored layers in probably similar sediments above or elsewhere. For example, Horn et al. (1969) reported that white volcanic ash in the northeast Pacific ranged in thickness from 1 to 29 cm (avg. 6.5 cm); the thicker sections would be those closest to sources of the ash; the mean grain size of these ashes was 5.42 phi. Similar information is usually available in the literature (e.g., Horn et al., 1971).

The alternatives when computing true thicknesses of relatively thick sediment and rock layers in areas where no interval velocities have been measured was discussed in the main text.

A growing and important source of information on sediment and rock layers, and their properties, are the Initial Reports of the Deep Sea Drilling Project. These reports should always be consulted when compiling geoacoustic models in deep-sea areas.

SEDIMENT TYPE, MEAN DIAMETER OF MINERAL GRAINS, and PERCENTAGES OF SAND, SILT, AND CLAY were determined from grain size analyses. These follow the nomenclature scheme discussed by Shepard, 1954; however, the Wentworth scale was used for sand sizes. The Wentworth scale is based on median diameter of mineral grains; very fine sand (0.062 to 0.125 mm); fine sand (0.125 to 0.250 mm); medium sand (0.250 to 0.500 mm); coarse sand (0.500 to 1.000 mm); silt (0.062 to 0.004 mm); and clay (less than 0.004 mm).

POROSITY is the volume of voids or pore space divided by the volume of the sample; this was determined from evaporation of pore water and corrected for dried salts (see Hamilton, 1971b for methods).

DENSITY OF SOLIDS, the bulk density of the mass of dried mineral grains (without salts evaporated from the pore water), was determined by the pycnometer method.

Total thickness of sediment over rock (in the footnote) was determined from one-way reflection time in the sediment and sediment interval velocity as discussed above.

Table B.3 In Situ Acoustic Properties of Sediments

SOUND VELOCITY was determined in the laboratory at approximately 200 kHz, and corrected to in situ values (Hamilton, 1971b); the values in parentheses are predictions. (See the following paragraphs for velocities in the lower layers.)

VELOCITY GRADIENT. The linear velocity gradient (in meters per second per meter, or sec^{-1}) shows the increase in velocity with depth in the sediments. At those stations where interval velocities were measured with sonobuoys, the overall linear gradient was established by using the sediment-surface velocity and the layer-interval velocity. The interval velocity is the actual velocity at a depth in the sediment of one-half the layer thickness. These gradients are smoothed, average gradients through the whole layer or layers, and do not reflect the various velocities in individual layers; consequently, only one gradient is usually given or estimated. Lacking actual measurements, a gradient is predicted (in par-

entheses); see main text, or Hamilton et al. (1974) for a discussion. These linear gradients usually vary between 0.5 and 2.0 sec^{-1}; a reasonable, over-all prediction is 1.0 sec^{-1}.

For many stations, the tables should indicate estimated properties for lower layers. The estimate is made by relating the properties to those in a higher layer or by predicting sediment type and properties from similar sediments.

The total thickness of sediments in models required by acousticians varies with frequency, energy, grazing angle, etc. Consequently, the known layering can be alternated, as previously indicated, to the sediment-rock interface to furnish a rational basis for geoacoustic models in areas where layered turbidites are present. The velocity gradient should then be used to correct (increase) velocity in each lower layer, a procedure which requires that the impedance also be corrected. For example, assume a velocity of 1500 m/sec and a gradient of 1.0 sec^{-1} in layer 1. A similar layer at a depth of 100 m in the sediment body will have a velocity of 1600 m/sec.

VELOCITY RATIO is computed by dividing the sediment velocity by the bottom-water velocity; it is the same in the laboratory as in situ (Hamilton, 1971b). At greater sediment depths, the ratio is not given or estimated. If computations are made for deeper layers, the velocity gradient in the sediment must

be considered (see previous paragraphs).

DENSITY is the saturated bulk density of a unit volume of sediment, in situ, as corrected from laboratory measurements. Densities at deeper depths can be estimated with the appropriate curve of density versus depth (Figure 6).

IMPEDANCE is the product of the in situ values of density and velocity.

Table B.4 Predicted Attenuation of Compressional (Sound) Waves

A study by Hamilton (1972) indicated that attenuation of sound in marine sediments was approximately dependent on the first power of frequency. In the equation $\alpha = kf^n$ (where attenuation, α, is in dB/m and frequency, f, in kHz), if the exponent "n" is taken as one, the only variable is the constant "k". Relationships between k and mean grain size and porosity (Hamilton, 1972, figs. 3-5) in the sediment layers have been used to derive a value of k. This value (and the probable maximum and minimum values) can be substituted into the equation above to derive an equation which can be used at any frequency. Attenuation at depth in thicker layers can be estimated from Figure 18 and associated text discussion.

Table B.5 In situ, Computed Elastic Constants of Sediments

All these values were computed by using the measured density, measured compressional (sound) velocity, and a computed value for the bulk modulus (corrected to in situ conditions) with Equations (19) to (23); as discussed in the first part, and in Hamilton (1971a, b.).

Table B.1 In situ properties of bottom water.*

True Depth, m	T, °C	S, ppt	P, kg/cm^2	Sound speed, m/sec	Density, g/cm^3	Impedance, g/cm^{2}sec x 10^5
5251	1.58	34.69	547.4	1546.6	1.05174	1.62662

* At location of model: coring site

Table B.2. In situ physical properties of sediments (other than acoustic).*

Layer No.	h, m	Sediment type	Mean Diam., mm	Sand, %	Silt, %	Clay, %	n, %	ρ_s, g/cm^3
1	6.2	Silty clay	0.004	9.8	39.0	51.2	76.3	2.65
2	0.1	(Volcanic ash)	—	—	—	—	(65.0)	(2.7)
3	3.0	(Silty clay)	—	—	—	—	(75.0)	(2.65)
4	0.2	(Volcanic ash)	—	—	—	—	(65.0	(2.7)
Rock	—	Basalt	—	—	—	—	—	—

Total thickness of sediment over rock: 100m

* At location of model: coring site.

Notes

(1) Column headings: h is thickness; n is porosity; ρ_s is density of solids.

(2) Values in parentheses are predicted.

(3) For a complete, estimated geoacoustic model, assume alternation of Layers 3 and 4 to full thickness of sediment (100m).

(4) Rock type (basalt) determined from velocity, acoustic reflection records (traced into seamounts), and Deep Sea Drilling Project in general area.

Table B.3 In situ acoustic properties of sediments.*

Layer No.	Sound velocity, m/sec	Velocity gradient, sec^{-1}	Velocity ratio	Density, g/cm^3	Impedance, $g/cm^2 sec \times 10^5$
1	1539	(1.0)	0.994	1.44	2.216
2	(1595)	——	(1 03)	(1.63)	(2.600)
3	(1545)	——	——	(1.45)	(2.240)
4	(1598)	——	——	(1.63)	(2.605)
Rock	(5700)	——	——	(2.8)	(15.96)

* At location of model: coring site,

Notes

(1) Values in parentheses are predicted. Velocity increased in lower layers by the amount indicated by the velocity gradient.

(2) For a complete, estimated geoacoustic model, assume alternation of Layers 3 and 4 to full thickness of sediment (100 m). See notes for this table in Appendix B.

(3) Velocity in basalt from an average for the general area from Houtz et al., 1970. Density in basalt from velocity-density relationship of Christensen and Salisbury, 1975, table 9: DSDP basalts at a pressure of 0.5 kb.

Table B.4. In situ, computed elastic constants of sediments.*

Layer No.	β	κ	σ	μ	λ	V_s
1	0.3055	3.2736	0.484	0.1028	3.2051	267
2	0.2623	3.8128	0.468	0.2505	3.6457	392
3	0.3003	3.3298	0.485	0.0986	3.2641	261
4	0.2623	3.8128	0.466	0.2622	3.6379	401
Rock (Basalt)	0.017	58.48	0.317	24.37	42.24	2950
(See note below for derivation of rock properties)						

*Compressibility, β, dynes/cm^2 X 10^{-10}
Bulk modulus, κ, dynes/cm^2 X 10^{10}
Poisson's Ratio, σ
Rigidity modulus, μ, dynes/cm^2 X 10^{10}
Lamé's Constant, λ, dynes/cm^2 X 10^{10}

Shear-wave velocity, V_s, m/sec

Data and the method used to compute elastic constants of sediments are in

Hamilton, E. L., 1971a, Elastic properties of marine sediments, JOUR. GEOPHYS. RES., v. 76, p. 579-604.

Hamilton, E. L., 1971b, Prediction of in-situ acoustic and elastic properties of marine sediments, GEOPHYSICS, v. 36, No. 2, p. 266-284.

Note: Properties of the basalt were computed from V_p from Houtz et al. (1970); density and V_s from Christensen and Salisbury, 1975: table 9: DSDP basalt at pressure of 0.5 kb; and Equations (19) to (23).

Table B.5. Predicted attenuation of compressional (sound) waves.*

Layer No.	k		
	Recommended	Probable Max.	Probable Min.
1	0.08	0.18	0.04
2	0.12	0.38	0.09
3	0.08	0.19	0.04
4	0.12	0.38	0.09
Rock (Basalt)	0.03	0.05	0.02

* To determine an equation which can be used at any frequency, substitute k into the equation

$$\alpha = kf^1$$

where

α is attenuation of compressional (sound) waves in dB/m
k is a constant
f is frequency in kHz

For deeper layers, alternate values shown for Layers 3 and 4 and as discussed in text with Figure 18.

Data and the method used to predict attenuation are in

Hamilton, E. L., 1972, Compressional-wave attenuation in marine sediments, GEOPHYSICS, v. 37, No. 4, p. 620-646.

Acknowledgments

This work was supported by the Naval Sea Systems Command (Code 06H14), by the Naval Electronic Systems Command (Code 320), and by the Office of Naval Research (Code 483). R.T. Bachman, P.H. Sherrer, and A.J. Brescia assisted in data analyses.

REFERENCES

ADLER, F.T., SAWYER, W.M., and FERRY, J.D. Propagation of transverse waves in viscoelastic media. Jnl. Applied Physics 20, 1949: 1036-1041.

AKAL, T. The relationship between the physical properties of underwater sediments that affect bottom reflection. Marine Geology 13, 1972: 251-266.

ATTWELL, P.B., and RAMANA, Y.V. Wave attenuation and internal friction as functions of frequency in rocks. Geophysics 31, 1966: 1049-1056.

BALARISHNA, S., and RAMANA, Y.V. Integrated studies of the elastic properties of some Indian rocks. In: KNOPOFF, L., et al (eds). The Crust and Upper Mantle of the Pacific Area, Geophysical Monograph No. 12. Washington, D.C., American Geophysical Union, 1968: pp 489-500.

BARKAN, D.D. Dynamics of Bases and Foundations. New York, McGraw-Hill, 1962.

BARNES, B.B., et al. Geophysics applied to geotechnical problems in a marine environment, a case study: Monterey Bay, California. In: Environmental Res. Labs., Annual Report 1972-1973. Washington, D.C., Nat. Oceanic and Atmos. Admin., 1973.

BERZON, I.S., RATNIKOVA, L.I., and MITRONOVA, V.A. Shear waves reflected from a thin high-speed layer. In: BERZON, I.S. (ed). Propagation in Real Media. (English trans.) New York, Consultants Bureau, 1969: 154-162. [Originally published Moscow, Nauka Press, 1967].

BRADLEY, J.J., and FORT, A.N. Internal friction in rocks. In: CLARK, S.P. (ed). Handbook of physical constants, Memoir 97. New York, Geological Society America, 1966: pp 175-194.

BRESLAU, L.R. Classification of sea-floor sediments with a shipborne acoustical system. In: Le Petrole et la Mer, Proceedings of Symposium, Sect. I, No. 132. Monaco, 1965: pp 1-9.
Also in: WHOI. Collected Reprints 1965, Pt 2, No. 1678. Woods Hole, Mass., Woods Hole Oceanographic Institution, 1966.

BRESLAU, L.R. The normally incident reflectivity of the sea floor at 12 Kc and its correlation with physical and geological properties of naturally-occurring sediments. WHOI Ref. 67-16. Woods Hole, Mass., Woods Hole Oceanographic Institution, 1967.

BUCHAN, S., et al. The Acoustic and Geotechnical Properties of North Atlantic Cores, Vols. 1 and 2. Menai Bridge, North Wales, Univ. College of North Wales Marine Science Lab., 1971.

BUCHAN, S., McCANN, D.M., and SMITH, D.T. Relations between the acoustic and geotechnical properties of marine sediments. Quarterly Jnl. Engineering Geology 5, 1972: 265-284.

BUCKER, H.P. Normal-mode sound propagation in shallow water. Jnl. Acoustical Society America 36, 1964: 251-258.

BUCKER, H.P., et al. Reflection of low-frequency sonar signals from a smooth ocean bottom. Jnl. Acoustical Society America 37, 1965: 1037-1051.

CERNOCK, P.J. Sound velocities in Gulf of Mexico sediments as related to physical properties and simulated overburden pressures. Tech. Rpt. 70-5-T. Austin, Texas., Texas A & M University Oceanographic Dept., 1970.

CHRISTENSEN, N.I., and SALISBURY, M.H. Structure and constitution of the lower oceanic crust. Review of Geophysics and Space Physics 13, 1975: 57-86.

CLAY, C.S., and RONA, P.A. Studies of seismic reflections from thin layers on the ocean bottom in the western North Atlantic. Jnl. Geophysical Research 70, 1965: 855-869.

COLE, B.F. Marine sediment attenuation and ocean-bottom-reflected sound. Jnl. Acoustical Society America 38, 1965: 291-297.

CUNNY, R.W., and FRY, Z.B. Vibratory in situ and laboratory soil moduli compared. Soil Mechanics and Foundation Engineering 99, 1973: 1055-1076.

DAVIES, D. Dispersed Stoneley waves on the ocean bottom. Bull. Seismological Society of America 55, 1965: 903-918.

DE BREMAECKER, J.C., GODSON, R.H., and WATKINS, J.S. Attenuation measurements in the field. Geophysics 31, 1966: 562-569.

DICKINSON, G. Geological aspects of abnormal reservoir pressures in Gulf Coast Louisiana. Bull. American Association of Petroleum Geologists 37, 1953: 410-432.

EWING, J.I., and NAFE, J.E. The unconsolidated sediments in the sea. In: HILL, M.N. (ed). The Sea; Ideas and Observations on Progress in the Study of the Seas, Vol. 3: The Earth beneath the Sea. New York, Interscience, 1963: pp 73-84.

EWING, J.I., et al. North Pacific sediment layers measured by seismic profiling. In: KNOPOFF, L., et al (eds). The Crust and Upper Mantle of the Pacific Area, Geophysical Monograph No. 12. Washington, D.C., American Geophysical Union, 1968: pp 147-173.

EWING, J.I., HOUTZ, R.E., and LUDWIG, W.J. Sediment distribution in the Coral Sea. Jnl. Geophysical Research 75, 1970: 1963-1972.

EWING, M., HOUTZ, R.E., and EWING, J. South Pacific sediment distribution. Jnl. Geophysical Research 74, 1969: 2477-2493.

FERRY, J.D. Viscoelastic Properties of Polymers. New York, John Wiley and Sons, 1961.

FRY, J.C., and RAITT, R.W. Sound velocities at the surface of deep sea sediments. Jnl. Geophysical Research 66, 1961: 589-597.

GARDNER, G.H.F., WYLLIE, M.R.J., and DROSCHAK, D.M. Effects of pressure and fluid saturation on the attenuation of elastic waves in sands. Jnl. Petroleum Technology 16, 1964: 189-198.

GASSMANN, F. Uber die Elastizitat Poroser Medien. Vierteljahresschrift der Naturforschenden Gesellschaft in Zurich 96, 1951: 1-23.

GRIFFITHS, J.C. Scientific Method in Analysis of Sediments. New York, McGraw-Hill, 1967.

HAMILTON, E.L. Low sound velocities in high-porosity sediments. Jnl. Acoustical Society America 28, 1956: 16-19.

HAMILTON, E.L. Thickness and consolidation of deep-sea sediments. Bull. Geological Society America 70, 1959: 1399-1424.

HAMILTON, E.L. Shear wave velocities in marine sediments (abstract). Trans. American Geophysical Union 51, 1970a: 333.

HAMILTON, E.L. Sound velocity and related properties of marine sediments, North Pacific. Jnl. Geophysical Research 75, 1970b: 4423-4446.

HAMILTON, E.L. Sound channels in surficial marine sediments. Jnl. Acoustical Society America 48, 1970c: 1296-1298.

HAMILTON, E.L. Reflection coefficients and bottom losses at normal incidence computed from Pacific sediment properties. Geophysics 35, 1970d: 995-1004.

HAMILTON, E.L. Elastic properties of marine sediments. Jnl. Geophysical Research 76, 1971a: 579-604.

HAMILTON, E.L. Prediction of in-situ acoustic and elastic properties of marine sediments. Geophysics 36, 1971b: 266-284.

HAMILTON, E.L. Compressional-wave attenuation in marine sediments. Geophysics 37, 1972: 620-646.

HAMILTON, E.L. Prediction of deep-sea sediment properties: state of the art. In: INDERBITZEN, A.L. (ed). Physical and Engineering Properties of Deep-Sea Sediments, Proceedings of a Symposium. New York, Plenum Press, 1974a: pp 1-43.

HAMILTON, E.L. Geoacoustic models of the sea floor. In: HAMPTON, L.D. (ed). Physics of Sound in Marine Sediments, Proceedings of a Symposium. New York, Plenum Press, 1974b: pp 181-221.

HAMILTON, E.L. Acoustic and related properties of the sea floor; density and porosity profiles and gradients, Tech. Pub. in press. San Diego, Calif., Naval Undersea Center, 1975a.

HAMILTON, E.L. Acoustic and related properties of the sea floor: sound attenuation versus depth, Tech. Pub. in press. San Diego, Calif., Naval Undersea Center, 1975b.

HAMILTON, E.L. Acoustic and related properties of the sea floor: shear wave profiles and gradients, Tech. Pub. in press. San Diego, Calif., Naval Undersea Center, 1975c.

HAMILTON, E.L., et al. Acoustic and other physical properties of shallow-water sediments off San Diego. Jnl. Acoustical Society America 28, 1956: 1-15.

HAMILTON, E.L., et al. Velocities of compressional and shear waves in marine sediments determined in situ from a research submersible. Jnl. Geophysical Research 75, 1970: 4039-4049.

HAMILTON, E.L., et al. Sediment velocities from sonobuoys: Bay of Bengal, Bering Sea, Japan Sea, and North Pacific. Jnl. Geophysical Research 79, 1974: 2653-2668.

HAMPTON, L. (ed). Physics of Sound in Marine Sediments. New York, Plenum Press, 1974.

HANNA, J.S. Short-range transmission loss and the evidence for bottom-refracted energy. Jnl. Acoustical Society America 53, 1973: 1686-1690.

HASTRUP, O.F. Digital analysis of acoustic reflectivity in the Tyrrhenian Abyssal Plain. Jnl. Acoustical Society America 70, 1970: 181-190.

HORN, D.R., HORN, B.M., and DELACH, M.N. Correlation between acoustical and other physical properties of Mediterranean deep-sea cores, Tech. Rpt. 2. Palisades, N.Y., Lamont Geological Observatory, 1967.

HORN, D.R., HORN, B.M., and DELACH, M.N. Correlation between acoustical and other physical properties of deep-sea cores. Jnl. Geophysical Research 73, 1968: 1939-1957.

HORN, D.R., DELACH, M.N., and HORN, B.M. Distribution of ash layers and turbidities in the North Pacific. Bull. Geological Society America 80, 1969: 1715-1724.

HORN, D.R., et al. Turbidities of the Hatteras and Sohm Abyssal Plains, western North Atlantic. Marine Geology 11, 1971: 287-323.

HOUTZ, R.E. Preliminary study of global sediment sound velocities from sonobuoy data. In: HAMPTON, L.D. (ed). Physics of Sound in Marine Sediments, Proceedings of a Symposium. New York, Plenum Press, 1974b: pp 519-535.

HOUTZ, R.E., and EWING, J.I. Detailed sedimentary velocities from seismic refraction profiles in the western north Atlantic. Jnl. Geophysical Research 68, 1963: 5233-5258.

HOUTZ, R.E., EWING, J.I., and LePICHON, X. Velocity of deep-sea sediments from sonobuoy data. Jnl. Geophysical Research 73, 1968: 2615-2641.

HOUTZ, R.E., EWING, J.I., and BUHL, P. Seismic data from sonobuoy stations in the northern and equatorial Pacific. Jnl. Geophysical Research 75, 1970: 5093-5111.

IGARASHI, Y. In situ high-frequency acoustic propagation measurements in marine sediments in the Santa Barbara shelf, California, Tech. Pub. 334. San Diego, Calif., Naval Undersea Center, 1973.

INDERBITZEN, A.L. (ed). Deep-Sea Sediments, Physical and Mechanical Properties. New York, Plenum Press, 1974.

KAWASUMI, H., et al. S-wave velocities of subsoil layers in Tokyo, 1. Bull. Earthquake Research Institute, Univ. of Tokyo 44, 1966: 731-747.

KELLER, G.H., and BENNETT, R.H. Variations in the mass physical properties of selected submarine sediments. Marine Geology 9, 1970: 215-223.

KERMABON, A., BLAVIER, C.G.P., and TONARELLI, B. Acoustic and other physical properties of deep-sea sediments in the Tyrrhenian Abyssal Plain. Marine Geology 7, 1969: 129-145.

KINSLER, L.E., and FREY, A.R. Fundamentals of Acoustics 2nd ed. New York, John Wiley and Sons, 1962.

KNOPOFF, L., and MacDONALD, G.J.F. Attenuation of small amplitude stress waves in solids. Reviews of Modern Physics 30, 1958: 1178-1192.

KOLSKY, H. Stress Waves in Solids. New York, Dover Publ. Co., 1963.

KRIZEK, R.J. Application of the one-sided Fourier transform to determine soil storage and dissipation characteristics. In: Soil Structure Interaction, Proceedings of a Symposium. Tuscon, Univ. of Arizona, 1964:

KRIZEK, R.J., and FRANKLIN, A.G. Energy dissipation in a soft clay. In: Wave Propagation and Dynamic Properties of Earth Materials, Proceedings of a Symposium. Albuquerque, N.M. Univ. of New Mexico Press, 1968: pp 797-807.

KUDO, K., and SHIMA, E. Attenuation of shear waves in soil. Bull. Earthquake Research Institute., Univ. of Tokyo 48, 1970: 145-158.

LASSWELL, J.B. A comparison of two methods for measuring rigidity of saturated marine sediments, MS Thesis. Monterey, California, U.S. Naval Postgraduate School, 1970.

LAUGHTON, A.S. Sound propagation in compacted ocean sediments. Geophysics 22, 1957: 233-260.

Le PICHON, X., EWING, J., and HOUTZ, R.E. Deep-sea sediment velocity determination made while reflection profiling. Jnl. Geophysical Research 73, 1968: 2597-2614.

LEVYKIN, A.I. Longitudinal and transverse wave absorption and velocity in rock specimens at multilateral pressures up to 4000 kg/cm . Academy of Sciences USSR Bull (Izvestya) Physics of the Solid Earth (English ed.) 2, 1965: 94-98.

LUDWIG, W.J., HOUTZ, R.E., and EWING, M. Sediment distribution in the Bering Sea: Bowers Ridge, Shirshov Ridge, and enclosed basins. Jnl. Geophysical Research 76, 1971: 6367-6375.

LUDWIG, W.J., MURAUCHI, S., and HOUTZ, R.E. Sediments and structure of the Japan Sea. Bull. Geological Society America 86, 1975a: 651-664.

LUDWIG, W.J., HOUTZ, R.E., and EWING, J.I. Profiler-sonobuoy measurements in Columbia and Venezuela Basins, Caribbean. Bull. American Assn. Petroleum Geologists 59, 1975b: 115-123.

MAGARA, K. Compaction and migration of fluids in Miocene mudstone, Nagaoka Plain, Japan. Bull. American Assn. Petroleum Geologists 52, 1968: 2466-2501.

McCANN, D.M. Measurement of the acoustic properties of marine sediments. Acustica 26, 1972: 55-66.

McCANN, C., and McCANN, D.M. The attenuation of compressional waves in marine sediments. Geophysics 34, 1969: 882-892.

McDONAL, F.J., et al. Attenuation of shear and compressional waves in Pierre shale. Geophysics 23, 1958: 421-439.

MEISSNER, R. P-and SV-waves from uphole shooting. Geophysical Prospecting 13, 1965: 433-459.

MOLOTOVA, L.V. Velocity dispersion of body waves in terrigenous rocks. Academy of Sciences USSR Bull. (Izvestiya) Physics of the Solid Earth (English ed.) 7, 1965: 500-506.

MORRIS, H.E. Bottom-reflection-loss model with a velocity gradient. Jnl. Acoustical Society America 48, 1970: 1198-1202.

MORTON, R.W. Sound velocity in carbonate sediments from the Whiting Basin, Puerto Rico. Marine Geology 19, 1975: 1-17.

MUIR, T.G., and ADAIR, R.S. Potential use of parametric sonar in marine archeology, unpublished manuscript. Austin, Texas, Applied Research Laboratory, 1972.

NAFE, J.E., and DRAKE, C.L. Variation with depth in shallow and deep water marine sediments of porosity, density and the velocities of compressional and shear waves. Geophysics 22, 1957: 523-552.

NAFE, J.E., and DRAKE, C.L. Physical properties of marine sediments. In: HILL, M.N. (ed). The Sea; Ideas and Observations on Progress in the Study of the Seas, Vol. 3: The Earth beneath the Sea. New York, Interscience, 1963: pp 794-815.

NAFE, J.E., and DRAKE, C.L. Physical properties of rocks of basaltic composition. In: HEES, H.H. and POLDERVAART, H. (eds). Basalts. New York, Interscience Publ., 1967: pp 483-502.

NAVOCEANO. Handbook of Oceanographic Tables, SP-68. Washington D.C., U.S. Naval Oceanographic Office, 1966.

NEPROCHNOV, Yu. P. Seismic studies of the crustal structure beneath the seas and oceans. Academy of Science USSR Oceanology (English ed.) 11, 1971: 709-715.

NOLLE, A.W., and SIECK, P.W. Longitudinal and transverse ultrasonic waves in synthetic rubber. Jnl. Applied Physics 23, 1952: 888-894.

RICHART, F.E., WOODS, R.D., and HALL, J.R. Vibrations of Soils and Foundations. New Jersey, Prentice-Hall, 1970.

RIEKE, H.H., and CHILINGARIAN, G.V. Compaction of Argillaceous Sediments. New York, Elsevier, 1974.

SCHREIBER, B.C. Sound velocity in deep-sea sediments. Jnl. Geophysical Research 73, 1968: 1259-1268.

SEED, B.H., and IDRISS, I.M. Analyses of ground motions at Union Bay, Seattle during earthquakes and distant nuclear blasts. Bull. Seismological Society America 60, 1970: 125-136.

SHEPARD, F.P. Nomenclature based on sand-silt-clay ratios. Jnl. Sedimentary Petrology 24, 1954: 151-158.

SHIMA, E., et al. S-wave velocities in subsoil layers in Tokyo. 3. Bull. Earthquake Research Institute, Univ. of Tokyo 46, 1968: 1301-1312.

SHUMWAY, G. Sound speed and absorption studies of marine sediments by a resonance method, Parts I & II. Geophysics 25, 1960: 451-467 and 659-682.

SUTTON, G.H., BERCKHEIMER, H., and NAFE, J.E. Physical analysis of deep-sea sediments. Geophysics 22, 1957: 779-812.

TYCE, R.C. Near-bottom observations of 4 kHz acoustic reflectivity and attenuation, in press. Geophysics, 1975.

VASSIL'EV, Y.I., and GUREVICH, G.I. On the ratio between attenuation decrements and propagation velocities of longitudinal and transverse waves. Academy of Sciences USSR Bull. (Izvestiya) Geophysics (English ed.) 12, 1962: 1061-1074.

WARRICK, R.E. Seismic investigation of a San Francisco Bay mud site. Bull. Seismological Society America 64, 1974: 375-385.

WHITE, J.E. Seismic Waves: Radiation, Transmission, and Attenuation. New York, McGraw-Hill, 1965.

WHITE, J.E., and SENGBUSH, R.L. Velocity measurements in near-surface formations. Geophysics 18, 1953: 54-69.

WHITMAN, R.V., and RICHART, F.E. Design procedures for dynamically loaded foundations. Soil Mechanics and Foundation Engineering 93, 1967: 169-193.

WU, T.H. Soil Mechanics. Boston, Allyn and Bacon, 1966.